Università degli Studi di Roma Sapienza
Dipartimento di Chimica- Stanislao Cannizzaro
Centro Nazionale Ricerche.
Istituto di Struttura della Materia.

E D X D 2006

ENERGY DISPERSIVE X-RAY TECHNIQUES

IN

CHEMICAL, PHYSICAL AND BIOLOGICAL RESEARCH

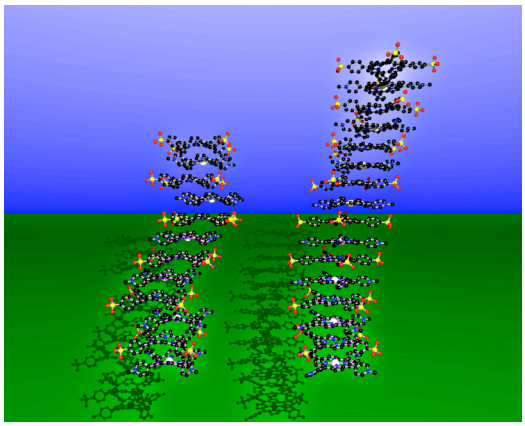

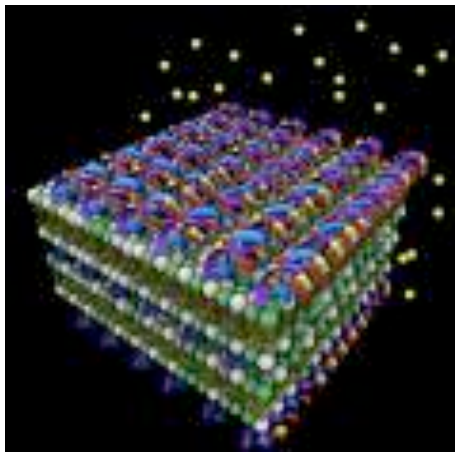

Prof. Ruggero Caminiti

Università degli Studi di Roma
Sapienza

Dipartimento di Chimica- Stanislao Cannizzaro

Prof. Ruggero Caminiti

ENERGY DISPERSIVE X-RAY TECHNIQUES

IN

CHEMICAL, PHYSICAL AND BIOLOGICAL RESEARCH

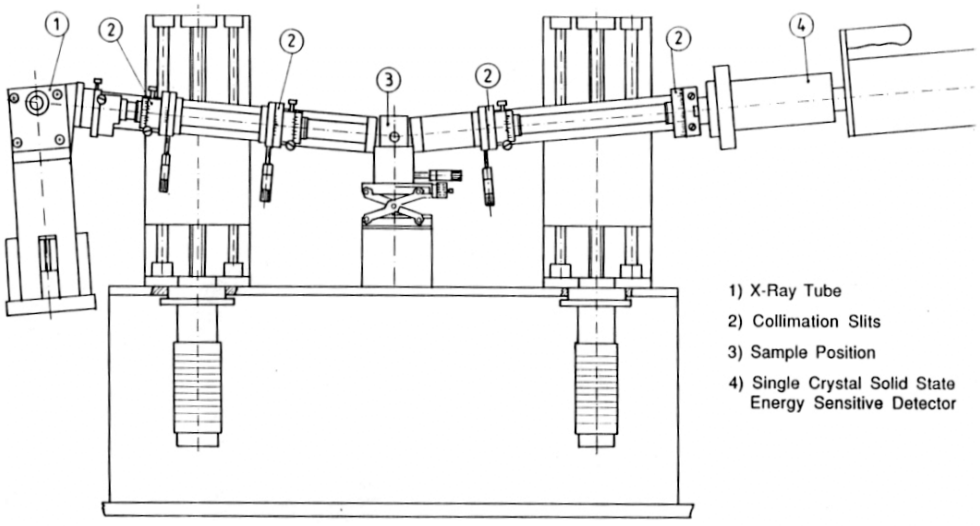

Edited by Ruggero Caminiti

Contents

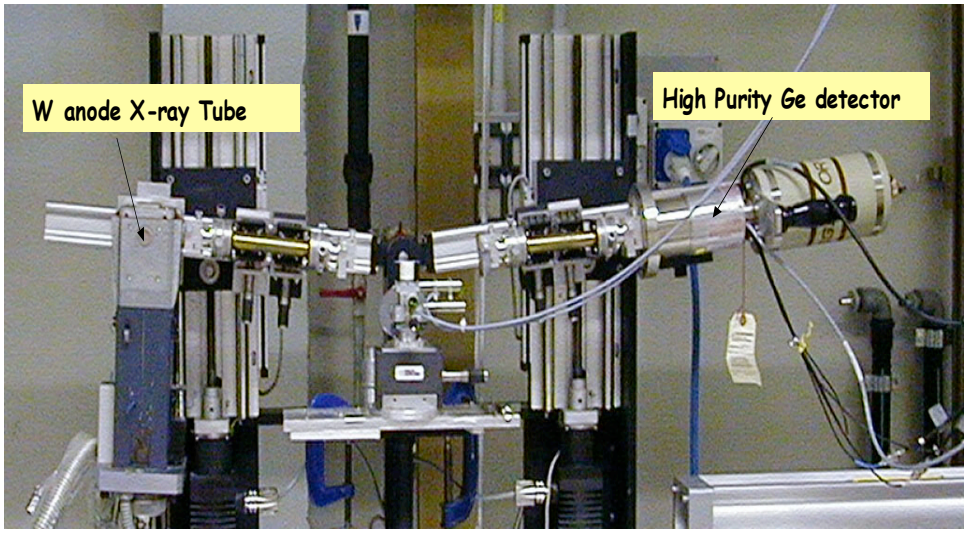

General Information

Location

Prof. Ruggero Caminiti
Dipartimento di Chimica –Stanislao Cannizzaro-Università Sapienza
P.le Aldo Moro 5 I-00185 Roma (Italy)
mail: r.caminiti@caspur.it; tel 06 49913661

Prof. Paolo Ballirano:
Dipartimento di Scienza della Terra - Università Sapienza
P.le Aldo Moro 5 I-00185 Roma (Italy)
mail: paolo.ballirano@uniroma1.it; tel 06 49914976

Dott. Giulio Caracciolo
Dipartimento di Chimica –Stanislao Cannizzaro-Università Sapienza
P.le Aldo Moro 5 I-00185 Roma (Italy)
mail: g.caracciolo@caspur.it; tel 06 49913076

Dott.ssa Amanda Generosi:
Istituto di Struttura della Materia – Consiglio Nazionale delle Ricerche
Area di Ricerca di Tor Vergata, Via del Fosso del Cavaliere 100, I-00133 Roma
mail: amanda@ism.cnr.it; tel 06 49934146

Dott. Lorenzo Gontrani
Consorzio Interuniversitario per le Applicazioni di Supercalcolo per Università e Ricerca (C.A.S.P.U.R.)
Via dei Tizii, 6 – I-00185 Roma (Italy)
mail: l.gontrani@caspur.it, tel 06 44486812

Dott. Roberto Matassa:
Dipartimento di Chimica –Stanislao Cannizzaro-Università Sapienza
P.le Aldo Moro 5 I-00185 Roma (Italy)
mail: matassa_rob@hotmail.com; tel 06 49913076

Dott.ssa Daniela Pozzi
Dipartimento di Chimica –Stanislao Cannizzaro-Università Sapienza
P.le Aldo Moro 5 I-00185 Roma (Italy)
mail: d.pozzi@caspur.it; tel 06 49913076

Dott. Valerio Rossi Albertini
Istituto di Struttura della Materia – Consiglio Nazionale delle Ricerche
Area di Ricerca di Tor Vergata, Via del Fosso del Cavaliere 100, I-00133 Roma
mail: valerio.rossi@ism.cnr.it; tel 06 49934146

Characteristics of the EDXD Technique

Ruggero Caminiti

In the EDXD technique, a continuous energy spectrum radiation is used as primary beam. Each chromatic component must, therefore, be analysed separately, taking into account all the energy-dependent effects that accompany the elastic scattering, such as absorption, polarization, inelastic scattering.

Along with such undesired effects due to the way of production of X-rays (namely, the polarization) and their interaction with the sample (absorption and inelastic scattering), a further effect induced by the detection process must be taken into account, that is a deformation of the spectral profile produced by the fluorescence of the X-ray sensible crystal ('escape peaks').

To perform an absolute measurement all the energy dependent quantities have to be measured or, at least, calculated.

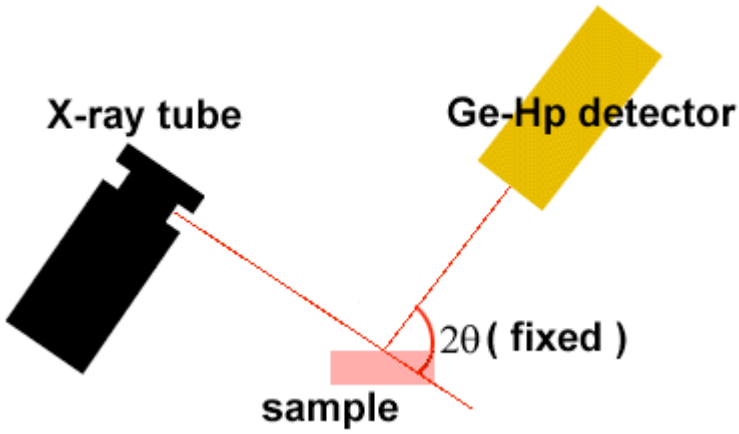

Moreover, in order to obtain an accurate measurement of the static structure factor from the diffracted intensity pattern, the q-range should be as wide as possible. Even if at a fixed angle a considerable portion($\Delta q \sim 4\text{-}5$ $Å^{-1}$) of the diffraction pattern can be collected, for an accurate structural study four diffraction patterns at different fixed angles must be usually collected and linked together to reproduce the whole diffraction spectrum.

The principle of EDXD is based upon the dependence of the scattering parameter **q** on two experimental variables: **E,** the incident beam energy and Θ, the diffraction angle: $q = (4\pi / hc) E \sin \Theta$.

As a consequence two methods are available to scan the reciprocal space: the angular dispersive one, which consists of fixing the radiation energy (i. e. using a monochromatic beam) and performing an angular scan. Reversely, one could fix the diffraction angle and execute an energy scan electronically, making use of a polychromatic radiation as the primary beam. In the latter case, the scan is carried out electronically (rather than mechanically as in the angular dispersive mode) by an energy dispersive solid state detector.

The q-range of the measured spectrum depends on the choice of Θ and on the spectral range of the source. The q resolution is related to the energy resolution provided by the solid state detector, typically a few hundred **eV** in the hard X-ray range, which must be added to the geometric contribution due to the angular spread.

A new energy-dispersive X-ray diffraction (EDXD) method to study the kinetics of the phase transitions (PTs) is reviewed. It enables one to follow the evolution of systems undergoing structural transformations in real time. It is based on a novel approach to PTs and provides several advantages with respect to the conventional techniques used for the same purpose. A detailed treatment of the theory is accomplished to demonstrate the consistency and reliability of this method. Despite the initial complexity of the subject that involves the interactions between X-ray and matter, just very simple measurements are required. Furthermore, the data processing is trivial and the relevant information on the PTs can be straightforwardly obtained from the X-ray spectra. The applications of the EDXD-PT method to the systems studied until now, namely polymeric, biological and mineralogical samples, are finally reported.

OFFERTA FORMATIVA

Disponibilità di tesi in Biofisica
sui seguenti argomenti

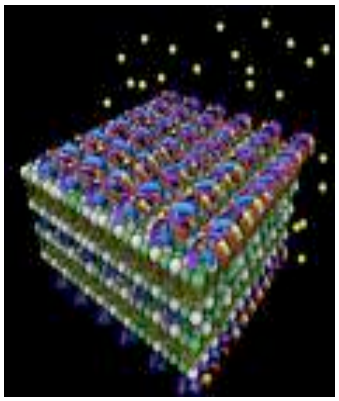

1.Interazione Lipoplessi-Membrane cellulari: Mescolando DNA e liposomi cationici (vescicole fatte di doppi strati lipidici concentrici e monostratidi acqua) in soluzione acquosa, si formano spontaneamente complessi liposoma/DNA (lipoplessi). Nell'ambito delle strategie di trasporto genico non virale, i lipoplessi rappresentano i vettori del DNA largamente più efficienti e biocompatibili. A dispetto del largo uso dei lipoplessi fatto in applicazioni di trasporto genico in vitro ed in vivo, i meccanismi molecolari di formazione dei lipoplessi, l'interazione di questi ultimi con la membrana cellulare ed il seguente rilascio del DNA risultano ancora poco compresi. Lo scopo della tesi è quello di chiarire i meccanismi chimico-fisici di interazione lipoplesso-membrana cellulare che presiedono al rilascio del DNA extracellulare nel citoplasma della cellula. Tale comprensione è il requisito necessario per razionalizzare l'efficienza dei lipoplessi e l'ingegnerizzazione di sistemi a multicomponenti lipidiche. Verranno condotti esperimenti di diffrazione X a basso angolo con luce di sincrotrone per studiare l'interazione lipoplesso-membrana cellulare, misure di elettroforesi su gel di agarosio per quantificare il rilascio del DNA ed esperimenti di trasfezione cellulare *in vitro* e *in vivo* per valutare l'attività delle diverse formulazioni lipidiche.

2. Formazione di lipoplessi su supporto-solido: l'obiettivo della tesi è quello di preparare lipoplessi orientati su supporto solido potenzialmente utili per lo *storage* di materiale genetico. La formazione dei lipoplessi e la successiva idratazione verranno seguiti mediante esperimenti EDXD *time-resolved*. L'utilizzo di molecole lipidiche diverse (lunghezza e saturazione delle code idrofobiche, proprietà chimico-fisiche delle teste polari etc.) consentirà di investigare dettagliatamente il meccanismo di formazione dei complessi (polarizzazione della carica elettrica, formazione di *lipidrafts* etc.).

3. Cinetiche di Idratazione di membrane lipidiche orientate su supporto solido: l'obiettivo della tesi è quello di studiare i fenomeni che avvengono a livello molecolare (distensione delle catene aciliche, protrusione delle teste polari nello strato di acqua inter-membrana, interazioni dipolari, etc.) a seguito dell'idratazione di doppi strati lipidici orientati su supporto solido attraverso esperimenti EDXD time-resolved. L'idratazione avviene *in situ* utilizzando una camera di idratazione opportunamente realizzata. Dal calcolo dei profili di potenziale repulsivo inter-membrana ci si aspetta di chiarire la natura della '*forza di idratazione*' tra membrane lipidiche.

Queste tesi saranno basate su dati raccolti nel laboratorio EDXD del Dipartimento di Chimica (**Tesi 2 e 3**) e/o presso la SAXS beamline della facility di Luce di Sincrotrone di Elettra (Trieste) o presso la beamline ID02 della facility di luce di sincrotrone ESRF (Grenoble, Francia) (**Tesi 1**).

Contatti: Prof. Ruggero Caminiti

Dott. Giulio Caracciolo

Dott.ssa Daniela Pozzi

Disponibilità di tesi di laurea e di dottorato in Scienza dei Materiali
presso il laboratorio di Raggi X dell'Istituto di Struttura della Materia del C.N.R., area della ricerca di Tor Vergata, sui seguenti argomenti

1.Caratterizzazione Strutturale *in-situ* di Membrane a conduzione protonica in celle a combustibile: Si offre la possibilità di svolgere tesi di laurea e/o dottorato basate sull'utilizzo di tecniche di Diffrazione di Raggi-X in dispersione di energia (EDXD) su membrane a conduzione protonica. Tali membrane rappresentano l'elemento caratterizzante delle celle a combustibile polimeriche (PEM-fuel cells) essendone lo scambiatore protonico e determinandone le risposte in termini di prestazioni (efficienza, durata, rendimento, etc.). La caratterizzazione strutturale di tali membrane e la variazione di tale struttura durante il funzionamento di una cella, in dipendenza dei diversi gradi di idratazione della membrana medesima, della temperatura di esercizio, della corrente di cella etc., rappresentano lo scopo ultimo di questi studi. Tali informazioni, essenziali per lo sviluppo e l'ottimizzazione di queste nuove fonti di energia rinnovabile, saranno ricavate attraverso misure EDXD risolte nel tempo ed eseguite *in-situ* sul sistema ingegnerizzato (cella a combustible completa e funzionante) e non (membrane singole).

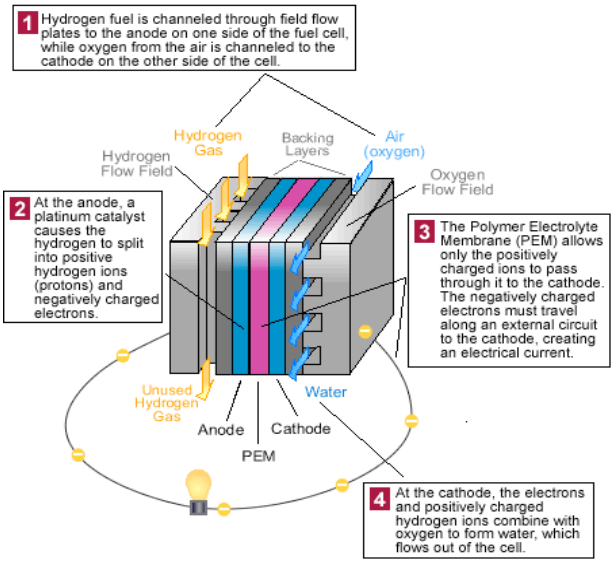

Principio di funzionamento di una cella a combustibile

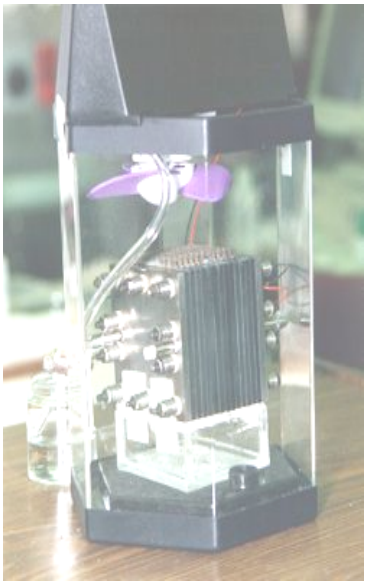

Aspetto di una cella commerciale

2. Studi di Riflettometria di Raggi-X sugli elementi attivi di celle solari organiche: Lo sviluppo di moderne celle solari, superata la vecchia concezione basata sull'utilizzo di semiconduttori come il Silicio, si rivolge oggi verso materiali plastici, alla ricerca di sistemi più economici, versatili e che, allo stesso tempo, abbiano rendimenti confrontabili con quelli ottenuti da le celle solari di vecchia concezione. Mediante l'utilizzo della Riflettometria di raggi-X in dispersione d'energia (EDXR), tecnica in grado di investigare superfici ed interfacce, si propone uno studio basato sulla caratterizzazione degli elementi costituenti celle solari plastiche ingegnerizzate (complete e funzionanti). Attraverso l'analisi morfologica selettiva delle interfacce tra i componenti della cella (elettrodi, polimeri fotoassorbitori, materiali di contatto etc.) e delle loro superfici libere (celle parzialmente assemblate), e sfruttando la possibilità di eseguire misure risolte nel tempo ed in-situ, si intendono studiare le variazioni morfologiche responsabili degli invecchiamenti, delle cadute di prestazioni, delle perdite di efficienza (ad es: durante l'illuminazione). Oltre all'utilizzo della EDXR si prevedono studi di Microscopia a Forza Atomica (AFM) per una caratterizzazione morfologica ulteriore dei materiali attivi del dispositivo.

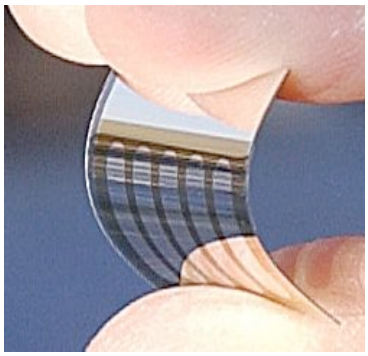

Celle solari organiche, leggere e flessibili

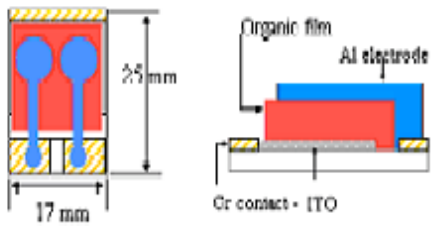

Schema di una cella solare studiata nel nostro laboratorio

Lo sviluppo di questa tematica avverrà presso i laboratori di Raggi X dell'Istituto di Struttura della Materia, C.N.R., area della ricerca di Tor Vergata.

3. Studio dell'interazione tra gas inquinanti e materiali sensibili per lo sviluppo si sensori: Attraverso l'utilizzo della Riflettometria di Raggi-X in Dispersione di Energia (EDXR) si investiga la natura delle interazioni chimico-fisiche alla base dei processi di risposta sensoristica di film sottili metallo-organici nei confronti gas inquinanti (es: NO/NO_2 vs Metallo-ftalocianine, VOC vs. Metallo-ftalocianine, gas ossidanti vs. porfirazine/metallo porfirazine). Tali interazioni sono spesso di diversa natura (superficiale, di bulk…) ed influenzano la qualità della risposta dei materiali come potenziali sensori per l'inquinamento atmosferico, modificando la loro sensibilità, selettività, reversibilità, durata etc. La determinazione della natura delle interazioni alla base dei processi di risposta sensoristica è l'obbiettivo di queste indagini. Lo scopo ultimo è di sviluppare materiali ingegnerizzabili come sensori ambientali. Si prevede l'utilizzo di tecniche di misura congiunte, cioè l'EDXR per l'indagine strutturale sui film sottili e conduttometriche, per lo studio delle proprietà di trasporto elettrico del dispositivo. Le misure saranno eseguite in tempo reale ed *in-situ* (ovvero durante l'interazione gas/materiale), e corredate con studi di microscopia a forza atomica (AFM) per la caratterizzazione delle proprietà superficiali dei sensori.

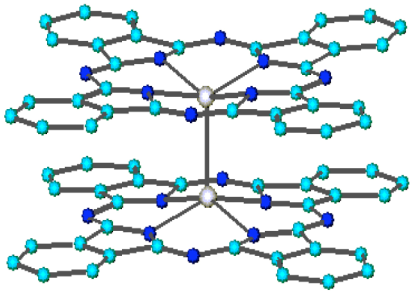

Struttura del materiale sensibile
(Metalloftalocianine)

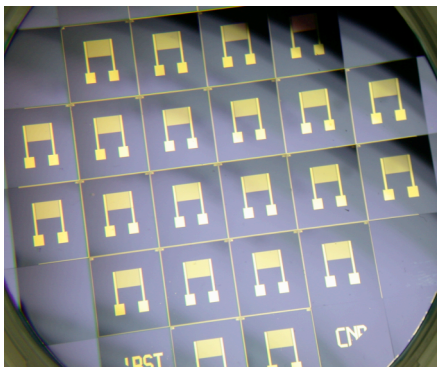

Supporti realizzati con fotolitografia
Ogni riquadro è costituito da un insieme
di minuscoli percorsi conduttori affiancati

Contatti: Dott. Valerio Rossi Albertini

Dott.ssa Amanda Generosi,

Dott.ssa Barbara Paci

Disponibilità di tesi in Chimica Fisica dello stato liquido

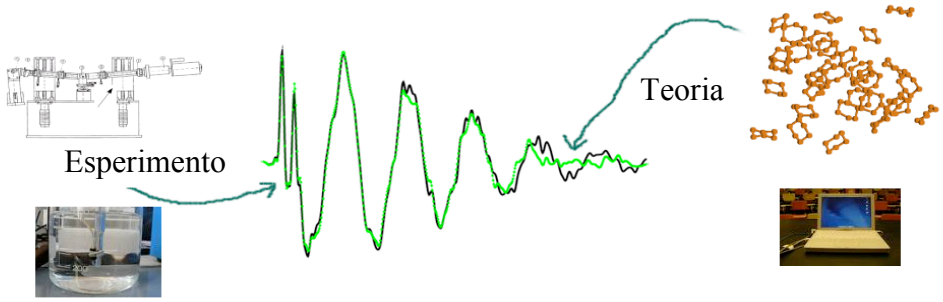

Lo stato liquido è di sicuro il più importante in chimica (quasi la totalità delle reazioni chimiche vengono effettuate in soluzione) e in biologia (come potrebbero esistere i biosistemi senza acqua?). Ciò grazie alle sue peculiari caratteristiche (basti pensare alla struttura e alle proprietà fisiche dell'acqua, tuttora il liquido più studiato). Eppure, la ricerca per descrivere le proprietà dei sistemi in fase liquida è appena cominciata. La diffrazione a raggi X, e in particolare la tecnica EDXD, costituisce uno dei metodi principali per ricavare la "struttura" della fase liquida, ovvero come sono disposti reciprocamente le particelle (molecole, ioni, atomi) che la compongono. Per formulare i modelli interpretativi dei dati sperimentali ottenuti, si impiegheranno la dinamica molecolare e le simulazioni Monte-Carlo.

Possibili argomenti di tesi:

Studio strutturale di liquidi puri e soluzioni Obiettivo della tesi è lo studio delle soluzioni acquose di molecole organiche di interesse biologico, come, ad esempio, aminoacidi, basi azotate. Le tesi saranno basate su dati raccolti nel laboratorio EDXD del Dipartimento di Chimica, e su calcoli teorici effettuati presso il dipartimento, in collaborazione con il centro di supercalcolo C.A.S.P.U.R. Verranno costruiti modelli di interazione molecola-molecola e/o molecola-solvente a diversa scala, impiegando le tecniche computazionali più adatte, dal calcolo *ab initio* (eventualmente tenendo conto degli effetti di volume (*bulk*) mediante metodi continui, come il PCM) alle simulazioni di dinamica classica (*Molecular Dynamics*). Se necessario, si costruirà un campo di forze (*force field*) opportuno per descrivere al meglio le interazioni.

Contatti: Dott. Lorenzo Gontrani

Disponibilità di tesi in Mineralogia

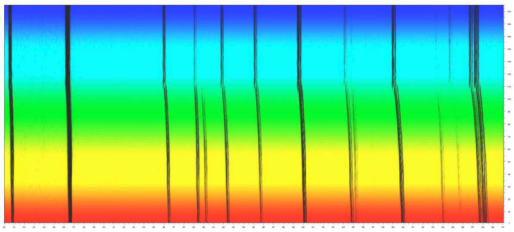

sui seguenti argomenti:

1 **Stabilità termica di solfati di calcio**: I solfati di calcio di formula generale $CaSO_4 \cdot nH_2O$ ($0 < n < 2$) sono fasi estremamente importanti in quanto costituenti naturali di imponenti formazioni evaporitiche, presenti anche in Italia, oltre che componenti fondamentali all'interno dei processi produttivi e alterativi dei cementi. Espansioni volumetriche elevate possono pregiudicare la stabilità di costruzioni civili ed impedire l'utilizzo di aree costituite da tali materiali come siti per la immobilizzazione di rifiuti nucleari. D'altro canto la presenza di una o dell'altra specie può modificare significativamente le proprietà reologiche del cemento. Scopo delle tesi è:

a Definire il numero ed il tipo di fasi a composizione $CaSO_4$ nH_2O ($0.5<n<1$), in quanto non si hanno ancora dati strutturali adeguati che confermino la loro presenza. Eventuale valutazione delle cinetiche di conversione da una forma all'altra. Queste fasi si presentano durante la preparazione di cemento Portland. Lo studio verrà effettuato utilizzando la diffrattometria RX su polveri a temperatura ambiente mediante un diffrattometro a fascio parallelo operante in trasmissione con rivelatore a stato solido.

b Studio della espansione termica e delle modificazioni strutturali indotte dalla temperatura sulle fasi a composizione $CaSO_4$ nH_2O ($0<n<2$). Lo studio verrà effettuato *in situ real-time* utilizzando la diffrattometria RX su polveri in condizioni non ambientali mediante un diffrattometro a fascio parallelo operante in trasmissione con rivelatore bidimensionale e prototipo di camera riscaldante per capillari.Le tesi saranno basate su dati raccolti presso il laboratorio di diffrazione RX avanzata su polveri del Dipartimento di Scienze della Terra e presso il laboratorio EDXD.

Contatti: Prof. Paolo Ballirano

Structural analysis of crystalline samples by the Rietveld method on laboratory EDXD data

Paolo Ballirano

The original development of a laboratory Energy-Dispersive system to analyse a crystalline specimen date back to the end of the 60s (Giessen & Gordon, 1968). Since then some applications of the Energy Dispersive X-ray Diffraction (EDXD) powder method on laboratory instruments have been reported despite the rather poor intrinsic relative resolution of the EDXD system that has severely limited its application in structural analysis. In fact, the relative resolution of an EDXD system is prevalently dominated by the contribution from the solid-state detector. Nevertheless, a few quantitative structural studies by means of EDXD on synchrotron sources have been reported (Glazer *et al*., 1978; Buras *et al*., 1979; Yamanaka & Ogata, 1991). Recently, the method is growing in popularity to monitor the evolution of lattice parameters with P and/or T in order to derive the corresponding equation of state or to detect the occurrence of phase

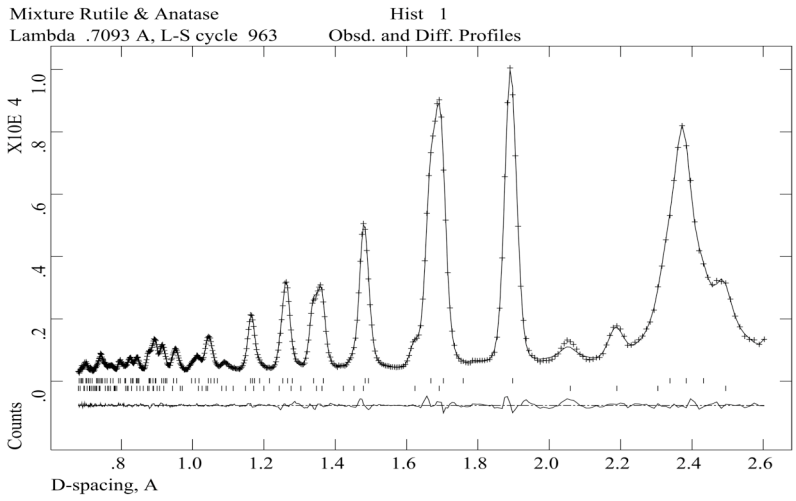

Experimental (dots) and calculated (continuous line) patterns of the synthetic mixture and anatase. Vertical markers: first row refers to the positionsof rutile of the calculated Bragg reflections for anatase; second row calculated Bragg reflections for rutile.

transitions (Zhang & Guyot, 1999). Both whole-pattern powder decomposition (Morishima *et al*., 1999) and Rietveld refinement (Frost & Fei, 1999) approaches have been applied to EDXD data but the aim being the refinement of the cell parameters. Only recently, this technique has been re-addressed toward laboratory instruments. In fact, our research group has recently investigated the possibility to perform, via Rietveld refinement (Rietveld, 1969), reliable structure analyses using laboratory EDXD data on fully crystalline samples [3,7].

Different materials have been selected according to increasing degrees of structural compexity and very different

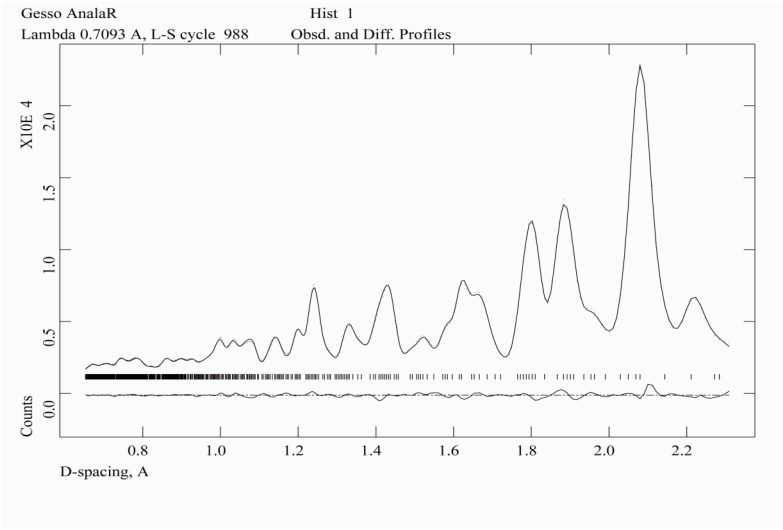

Experimental (dots) and calculated (continuous line) patterns of $CaSO_4 \cdot 2H_2O$ from the data set with 2000 s of counting time.

tendency to be affected by preferred anḍorientation (SRM676 Al2O3, synthetic mixture of nanocrystalline rutile anatase, gypsum CaSO4 · 2H2O). Samples were prepared as pellets of ca. 12 mm diameter and 1 mm of thickness. Measurements were performed, at a single Θ value, in symmetric-transmission geometry in order to simplify absorption correction procedures. Raw data were normalized to the incident white spectrum (fitted with a sixth-order polynomial) and corrected for absorption and escape peaks. Diffraction data were evaluated by the GSAS crystallographic package (Larson & Von Dreele, 1985). This suite of programs is, in fact, able to handle constant-*q* data by conversion to conventional ADXD data

using a fictitious, user-defined, wavelength ($MoK_{\alpha 1}$ = 0.70926 Å in this case). Peak shape was modeled using a pseudo-Voigt function (Thompson et al., 1987) modified for asymmetry (Finger et al., 1994) whereas the background was fitted with an eight term Chebyshev polynomial of the first kind. Structure refinements of Al2O3 lead to positional and displacement parameters reasonably close to those reported in single-crystal reference data, despite the low-resolution of the EDXD data. This is due to the significantly larger portion of reciprocal-space accessible by EDXD as compared to conventional ADXD. Moreover, the refinement of the data of the nanocrystalline TiO_2-polymorphs mixture has indicated a remarkable agreement between refined and nominal weight fractions (rutile: calculated wt% 18.0(4), nominal *ca*. 20%). Gypsum represented a more challenging test because of its greater structural complexity and a strong tendency to show texture effects. Reasonable structural results have been obtained for this material with collection times as short as 500 s. In fact, bond distances were within 1.5σ and angles within 1σ of both neutron (Pedersen & Semmingsen, 1982) and X-ray (Cole & Lancucki, 1974) reference single-crystal refinements. The larger discrepancy on bond lengths is taken up by the Ca-OH_2 bond distance that has been found to be systematically larger (*ca*. 0.04 Å) than the single-crystal value. This arises from the distortion, and corresponding displacement of the centre of gravity, of the electronic density of the oxygen atom of the water molecule because of the contribution of the two bonded hydrogen atoms. A counting time of 2000 s reduces the corresponding standard deviations to one half. This may be considered as a particularly satisfactory result especially because obtained via a completely unrestrained refinement and with a data set affected by significant preferred orientation.

More recently the Rietveld refinement has been applied to patterns collected at non-ambient conditions. The sample selected was polyethylene (PE) whose structural features were previously investigated (Caminiti *et al*., 2000) by means of conventional Angular Dispersive X-ray Diffraction (ADXD) at RT. A sample of approximately 20 x 20 x 2 mm has been fitted at the center of a thermostatic cell located at the optical centre of the goniometer.

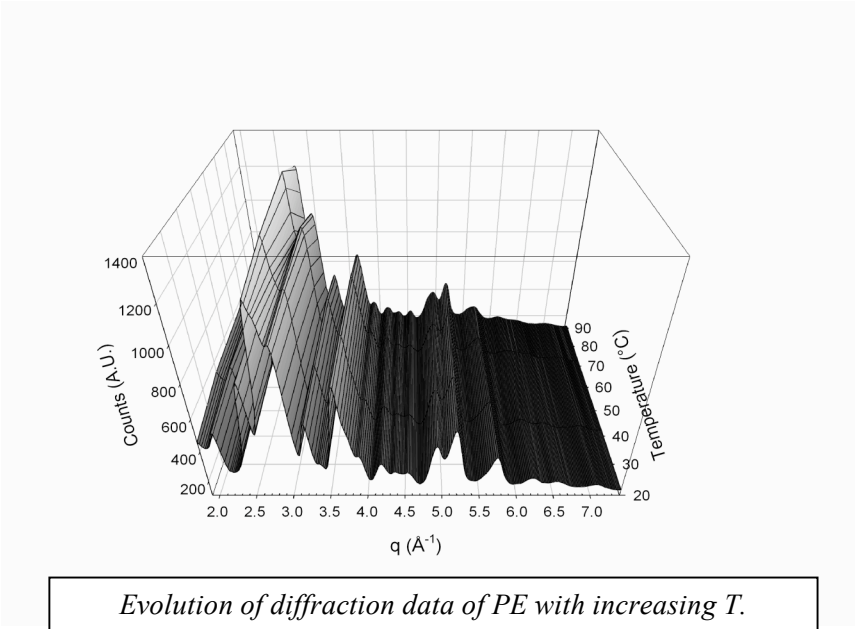

Evolution of diffraction data of PE with increasing T.

The measurement geometry was symmetric-transmission. The behavior has been studied at four temperatures, namely 25, 40, 70, and 88°C, below the melting point of the polymer. In this range the structure undergoes a regular volume expansion that may be expressed in terms of specific volume ratio as $V_E/V_{25°C} = 0.991(2) + 4.0(5)x10^{-4} * T(°C)$. The variation is almost completely due to the expansion of the *a* cell parameter and results, apart for minor intrachain arrangements, in an increased distance between polymer chains.

The results we have obtained so far are very promising because the instrument we used, at present, is not optimised for analysis of crystalline samples as it lacks soller slits. The use of these slits could permit a reduction of the axial divergence therefore improving the instrumental resolution. Although the EDXD technique is ideally suited for synchrotron sources as it takes full advantage of the properties of this X-ray source, laboratory instruments have the advantage of the availability. Moreover, whenever long experiments are involved, as in the case of real-time study of slow time-dependent phenomena, the emission stability of sealed tubes surpasses that of the storage rings.

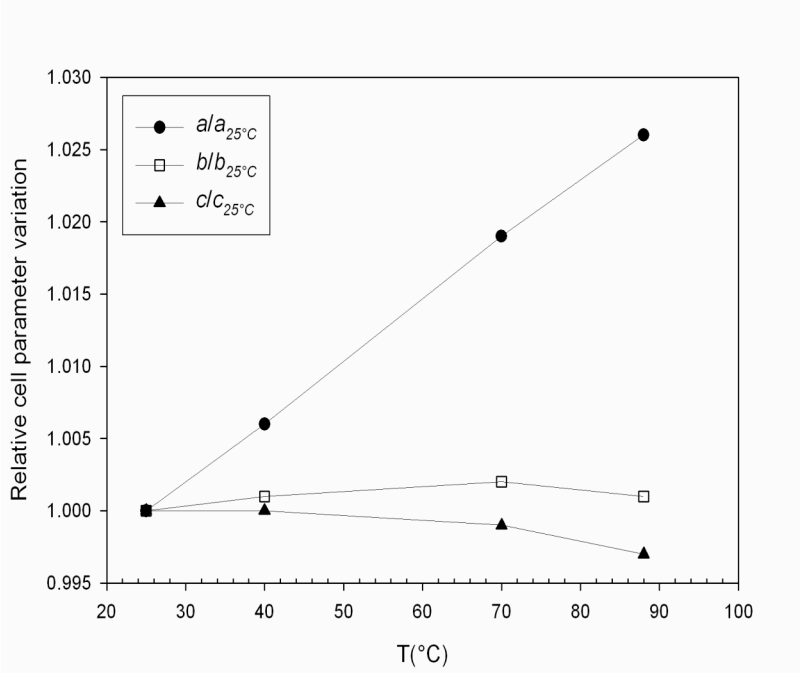

Relative cell parameters variation as a function of the temperature.

References

Buras, B., Gerward, L., Glazer, A.M., Hidaka, M., Staun Olsen, J. (1979). *J. Appl. Cryst*. **12**, 531-536.

Caminiti, R., Pandolfi, L., Ballirano, P. (2000).*J. M. Sci.-Phys*., B**39**, 481-492.

Cole, W.F. & Lancucki, C.J. (1974). *Acta Cryst*. B**30**, 921-929.

Finger, L.W., Cox, D.E., Jephcoat, A.P. (1994). *J. Appl Cryst*. **27**, 892-900.

Frost, D.J. & Fei, Y. (1999). *Phys. Chem. Minerals* **26**, 415-418.

Giessen, B.C. & Gordon, G.E. (1968). *Science* **159**, 973-975.

Glazer, A.M., Hidaka, M., Bordas, J. (1978). *J. Appl. Cryst*. **11**, 165-172.

Larson, A.C. & Von Dreele, R.B. (1985): *GSAS: General Structure Analysis System.* LAUR 86-748, Los Alamos National Laboratory, Copyright, 1985-1994, The Regent of the University of California.

Morishima, H., Ohtani, E., Kato, T., Kubo, T., Suzuki, A., Kikegawa, T. & Shimomura, O. (1999). *Phys. Chem. Minerals* **27**, 3-10.

Pedersen, B.F. & Semmingsen, D. (1982). *Acta Cryst*. B**38**, 1074-1077.

Rietveld, H.M. (1969). *J. Appl. Cryst*. **2**, 65-71.

Thompson, P., Cox, D.E., Hastings, J.B. (1987). *J. Appl. Cryst*. **20**, 79-83.

Yamanaka, T. & Ogata, K. (1991). *J. Appl. Cryst*. **24**, 111-118.

Zhang, J. & Guyot, F. (1999). *Phys. Chem. Minerals* **26**, 419-426.

POLYMERIC , CRISTALLINE STRUCTURES AND KINETICS

1) R. Caminiti, M. Gleria, K. B. Lipkowitz, G. M. Lombardo, G. C. Pappalardo
Molecular Dynamics Simulations Combined with Large Angle X-ray Scattering Technique For the Determination of the Structure, Conformation and Conformational Dynamics of Polyphosphazenes in Amorphous Phase: Study of Poly(di-(4-Methylphenoxy)Phosphazene).
J. Amer. Chem. Soc., 119(9), 2196-2204 (**1997**).

2) R. Caminiti, M. Gleria, K. B. Lipkowitz, G. M. Lombardo, G. C. Pappalardo
Molecular Modelling and Large Angle X-ray Scattering (E.D.X.D.) Studies of the Structure of Semicrystalline Poly[bis(phenoxy)phosphazene].
Chem. of Mat., 11(6), 1492-1497 (**1999**).

3) P. Ballirano, R. Caminiti
Rietveld refinements on laboratory energy dispersive X-ray diffraction (EDXD) data.
J. Appl. Cryst., 34, 757-762 (**2001**).

4) M.E. Amato, R. Caminiti, G. Carriedo, G. M. Lombardo, G. C. Pappalardo
Structural Features and Molecular Assembly of Amorphous Phosphazenic Materials in the Bulk. Combined Theoretical (Molecular Dynamics, MD) and Experimental (L.A.X.S., E.D.X.D.) Thechniques: Tris-(2,2'-dioxy-1,1'-binaphthyl) cyclotriphosphazene.
Eur. Inorg. J., 7, 1486-1494 (**2001**).

5) A. Isopo, R. Caminiti, R. D'Amato, A. Furlani and M. Vittoria Russo
Energy dispersive X-ray diffraction (EDXD) investigation of amorphous poly(phenylacetylene) (PPA).
J. Macromol. Sci. Phys. B, 1061-1083 (**2003**).

6) G. A. Carriedo, F. J. Garcìa Alonso, J. L. Garcìa Alvarez, G. M. Lombardo, G. C. Pappalardo, F. Punzo
Molecular Dynamics (MD) Simulations and Large-Angle X-ray Scattering (LAXS) Studies of the Solid-State Structure and Assembly of Isotactic (R)-Poly(2,2'-dioxy-1,1'-binaphthyl-) phosphazene in the Bulk State and in the Cast Film.
Chem. Eur. J., 10, 3775-3782 (**2004**).

7) R. Caminiti,P. Ballirano and M. Carbone
Polyethylene Structure as a Function of Temperature: An EDXD Investigation.
J. Macromol. Sci., Phys. B**45**, 1005-1014 (**2006**).

8) P. Ballirano, A. Maras, R. Caminiti, C. Sadun
Carbonate-cancrinite: In-situ real-time thermal processes studied by means of energy-dispersive X-ray powder-diffractometry.
Powder Diffraction, 10(3), 173 (**1995**).

9) R. Caminiti, C. Sadun, M. Bionducci, F. Buffa, G. Ennas, G. Licheri, A. Musinu, G. Navarra
Energy Dispersive x-ray diffraction applied to isothermal crystallization of the amorphous alloy Ni60B40.
Gazzetta Chimica, 127, 59-62 (**1997**).

10) P. Ballirano, R. Caminiti, C. Ercolani, A. Maras, M. A. Orrù
X-ray Powder Diffraction Structure Reinvestigation of the α and β Forms of Cobalt Phthalocyanine and in-situ Real-Time Kinetics of the α- β Phase Transition.
J. Amer. Chem. Soc., 120(49), 12798-12805 (**1998**).

11) G. A. Lehmann, M. Bionducci, F. Buffa
Effect of mechanical grinding on the hexagonal structure of CdSe.
Phys. Rev. B, 58(9), 5275-5281 (**1998**).

12) G. Ennas, G. Marongiu, A. Musinu, P. Ballirano, R. Caminiti
Characterization of Nanocrystalline γ-Fe2O3.Prepared by Wet Chemical Method.
J. Mater. Res., 14(4), 1570-1576 (**1999**).

13) B. Elsener, D. Atzei, A. Krolikoswski, V. Rossi Albertini, C. Sadun, R. Caminiti and A. Rossi
From Chemical to Structural Order of Electrodeposited Ni22P Alloy: An XPS and EDXD study.
Chem. Mater., 16(22), 4216-4225 (**2004**).

14) M. Carbone, P. Ballirano and R. Caminiti
A kinetic investigation of gypsum dehydration at reduced pressure by Energy Dispersive X-ray Diffraction(EDXD).
Eur. Mineral. J., (**2007**) *Submitted*.

Hydration effect on the structure of Dioleoylphosphocholine bilayers

Giulio Caracciolo

The interaction of water molecules with the lipid polar head groups is one of the fundamental aspects of biological membrane assembly.[1] Experiments with phospholipid model membranes have shown that the degree of head group hydration affects both the membrane structure and dynamics.[2-3] The molecular packing[4] and the interaction between bilayers[5] depend on the amount of water associated with the lipids. The chain melting phase transition and transformational to nonbilayer phases are also all dependent on water content. Although there have been various studies of lipid bilayers with saturated chains, there have been relatively few studies of lipid bilayers of unsaturated lipids, in particular, dioleoylphosphatidylcholine (DOPC) bilayers. X-ray diffraction studies of DOPC bilayers have previously focused on either low hydration[6]or full hydration[7] while Hristova and White[8] have studied DOPC bilayers at intermediate levels of hydration.

In this letter we report on the structural changes of oriented DOPC multibilayers induced by hydration. In this study, an experimental set-up that allows for *in situ* energy dispersive X-ray diffraction (EDXD) experiments with a precise control of relative humidity (RH) and temperature was used. The sample chamber, designed to overcome the experimental inadequacy that had previously led to the vapor-pressure paradox,[9] is elsewhere described.[10] In our investigation, we took specific advantage of using highly aligned lipid multibilayers which allow for more accurate diffraction analyses with respect to liposomic dispersions and are excellent model systems of biological membranes.[11]

DOPC was purchased from Avanti Polar Lipids (Alabaster, AL) and used without further purification. Oriented DOPC multibilayer stacks were prepared depositing 1 mg of lipid onto a flat freshly cleaved silicon wafer by evaporating from an isopropanol solution. After drying under a vacuum for 24 h, the sample was transferred to the hydration chamber. A single diffraction angle θ=1.06° was fixed

that allowed to cover simultaneously an overall region of the reciprocal space $0.092<q<1.1$ Å^{-1} (q=const×E×sinθ; const=1.014 Å^{-1} keV^{-1}).

DOPC multibilayers were hydrated trough vapor over the hydration range of 0.45–1 RH at constant temperature (T=300 K). In this region of the phase diagram (0.45<RH<1), DOPC membranes are in the liquid-crystalline L_α phase where the hydrocarbonic chains are melted while for RH<0.45 DOPC membranes are assembled in a three-dimensional rhombohedral R phase.[12] For 0.45<RH<0.7 (data not reported) we did not observe any appreciable structural change. At RH=0.7, the EDXD pattern of DOPC (not reported) exhibited five orders of sharp Bragg peaks (*00l*) indicating a high degree of translational order along the normal to the lipid bilayer and a lamellar periodicity $d=2\pi/q_{001}$=48.2 Å. This value was in close agreement with those already reported by us.[13] The electron density profile (EDP), $\Delta\rho(z)$, along the normal to the bilayers, z, was calculated as a Fourier sum of cosine terms as

$$\Delta\rho = \frac{\rho(z)-\langle\rho\rangle}{\left[\langle\rho^2(z)\rangle-\langle\rho\rangle^2\right]^{1/2}} = \sum_{l=1}^{N} F_l \cos\left(2\pi l\frac{z}{d}\right) \qquad (1)$$

where $\rho(z)$ is the electron density, $\langle\rho\rangle$ its average value, N is the highest order of the fundamental reflection observed in the EDXD pattern, F_l is the form factor for the (00*l*) reflection, d is the lamellar periodicity along the normal to the lipid bilayer consisting of one lipid bilayer and one water layer. The EDP was calculated with the appropriate phases (– – + – +).[14]

Fig. 1 shows the EDP along the normal to DOPC bilayers. The electron densities of the headgroups, ρ_H, and hydrocarbon tails, ρ_C, are defined relative to the methylene electron density ρ_{CH2} (Fig. 1, continuous line). According to recent definitions,[15] some water interacting intimately with the lipid membrane should be considered as a part of the structure itself. As a result, the headgroup size, d_H, can be estimated from the full width at half maximum (fwhm) of the Gaussian representing the headgroup (Fig. 1). As a result, the bilayer thickness is defined as the maximal thickness occupied by lipids thereby including water molecules associated with the hydration shell of lipid headgroups ($d_B=d_{HH}+d_H$).[15] According to geometric

considerations, further structural parameters are straightforward to be derived: the hydrocarbon core (HC) thickness, $d_C=(d_{HH}-d_H)$, and the thickness of the interbilayer water region, $d_W=d-d_B$.[15]

Fig. 1. Electron density profile along the normal to DOPC bilayers at relative humidity RH=0.7. The distance between the two electron density maxima defines the distance between the polar headgroups of DOPC molecules while the headgroup size, d_H, can be estimated from the full width at half maximum (fwhm) of the Gaussian representing the headgroup. The atoms of the DOPC molecules are colour-coded: H (white), C (green), N (cyan), P (pink), O (red).

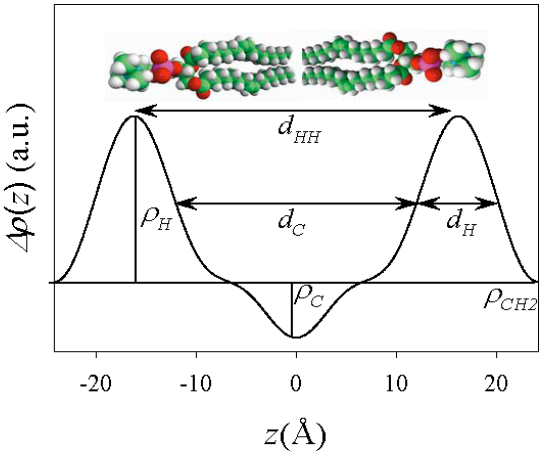

Fig. 2 shows the changes of structural parameters of DOPC bilayers as a function of RH. Two distinct regimes of hydration were identified. In the first regime (RH<0.94), the structure of DOPC bilayers was poorly sensitive to changes in hydration while, in the second one (0.94<RH<1), distinct structural changes were observed. The lamellar *d*-spacing and the thickness of the water layer, d_W, (Fig. 2, panels a and b, respectively) were found to swell almost linearly with RH up to RH~0.94 when an abrupt increase was detected. On the opposite, the membrane thickness (Fig. 2, panel c), d_B, firstly decreased, passed trough a minimum at RH~0.94 and then reached its maximum expansion at full hydration (d_B~40 Å). In first regime, the headgroup size, d_H, was not influenced, within experimental errors, by changes in hydration (d_H~4 Å, Fig. 2, panel d).

Fig.2. Structural parameters of DOPC bilayers as a funcion of RH.

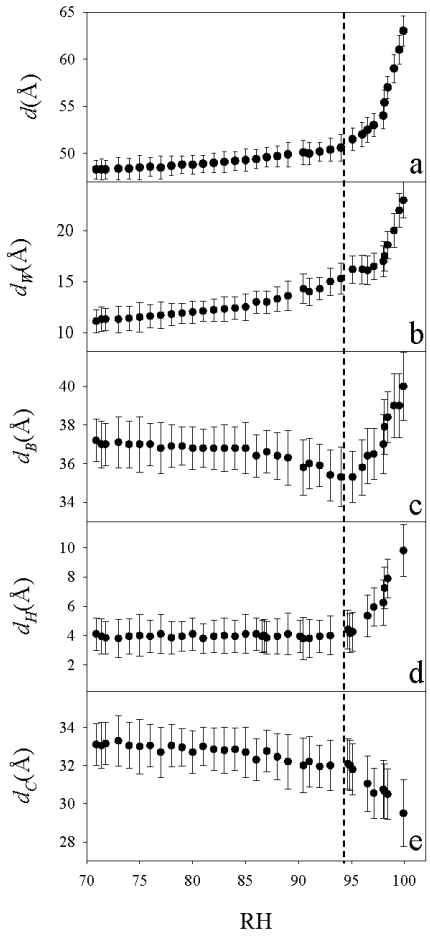

In the second regime, we found a strong expansion of the DOPC headgroup size up to RH=1 (d_H~9.8 Å). This value was found to be in excellent agreement with those reported, at full hydration, by McIntosh and Simon (10 Å)[16] and by Nagle and coworkers (9±1.2).[7] Structural analysis showed the protrusion of DOPC headgroups toward the interbilayer water region that accompanies increases in hydration. Structural **e**volution of d_C clarified how the hydrophobic core (HC) of DOPC bilayers changed with hydration (Fig. 2, panel e). In the first regime of hydration, flexibility of DOPC chains was slightly modified by hydration with reduction in HC thickness being less than 1 Å. At hydrations higher than RH=0.94 a marked thinning of the HC occurred as expected from the increased thermal motion of acyl chains that accompanies increased hydration. In more hydration, polar headgroups are associated by more water that enlarges the cross-sectional area in polar headgroup region, leaving empty space in hydrophobic region. The empty space is instantly filled up by flexible hydrocarbon chains, causing the bilayer thinning by hydration.

Our structural results raise a basic question: Which are the molecular mechanisms underlying experimental observations? Previously, Hristova and White[8] reported a study on the effect of hydration on the HC structure of DOPC bilayers and proposed the existence of a distinctive structural change upon completion of the DOPC hydration shell (d~50 Å; RH>0.93). Nevertheless, since the observed break in the Bragg spacing curve as a function of adsorbed waters also coincided with a change in the method of hydration, there was a concrete possibility, discussed by the authors, that it was an experimental artefact due to the change of the hydration protocol. In our study, we found a complete structural change (Fig. 2) occurring at RH~0.94 when the lamellar d-spacing was d~50.5 Å. So our findings confirmed the suggestions by Hristova and White. What is completely different in our EDXD experiments, is that only one lipid sample was used and that distinct hydrations were achieved inside the hydration chamber. We emphasize that the *in situ* EDXD measurements allowed a very high density sampling of the evolution of the structural properties of the DOPC bilayer.

Anyway, some further hypotheses can be made about the effect of hydration on the structure of DOPC bilayers. It is thought that, at low hydration, lipid molecules

interact with each other by electrostatic interactions between the headgroups. In the case of neutral DOPC, the phosphate group, which is linked to the glycerol backbone, has a negative charge while the choline group, which constitutes the free end of the headgroup, has a net positive charge. Upon hydration, the interaction between the lipid headgroups in the starting almost dry state is replaced by stronger water-headgroups H bonds between water and lipids. In fully hydrated membranes in the L_α phase, water molecules interact with the lipid headgroups and form bridges among them. We found that, for RH<0.94, the headgroup size along the normal to lipid bilayer is small (d_H~4 Å). This finding may suggest that P and N atoms lie in the plane of the membrane. This spatial organization of the P^- and N^+ atomic groups may allow pairs of DOPC molecules to interact with each other via P···N and N···P double pairs. For hydrations higher than RH=0.94, we found that the headgroup size along the normal to DOPC bilayer, increases up to d_H~9.8 Å. It is known that, upon hydration, water molecules fill the hydration shell of DOPC molecules thereby reducing the electrostatic interactions bwteeen P^- and N^+ atomic groups. Water molecules are polarized at the lipid-water interface and align their dipole moments toward the water bulk region thus creating a positive potential in the bilayer interior (where P atoms are located). N^+ atomic groups may therefore protrude toward the interbilayer water region to align the headgroup dipole moment (P→N vector) against the water dipole moment. In a recent simulation, Saiz and Klein[17] found that P^-atoms are located closer to the membrane interior than N^+ atoms. Thus, the microscopic origin of the observed swelling in the headgroup size (Fig. 2, panel d), may be the organization at the interface of the polar headgroups and the counteracting effect of the polarized hydrating water molecules.

References

[1]B. Bechinger and J. Seelig, Biochemistry **30**, 3923 (1991).

[2]H. Binder, T. Gutberlet, A. Anikin, and G. Klose, Biophys. J. **74**, 1908 (1998).

[3]J. N. Israelachvili and H. Wennerstrom, Nature Londond **379**, 219 (1996).

[4]J. N. Israelachvili and H. Wennerstrom, J. Phys. Chem. **96**, 520 (1992).

[5]R.P. Rand, and V.A. Parsegian, Biochim. Biophys. Acta **988,** 351 (1989).

[6]S.H. White and M. C. Wiener, Biophys. J. **61**, 434 (1992).

[7]S. Tristram-Nagle, H. I. Petrache, and John F. Nagle, Biophys. J. **75,** 917 (1998).

[8]K. Hristova, and S. H. White, Biophys. J. **74,** 2419 (1998).

[9]J. Katsaras, Biophys. J. **75,** 2157 (1998).

[10]G. Caracciolo, M. Petruccetti, and R. Caminiti,
Chem. Phys. Lett. **414**, 456 (2005).

[11]N. Kučerka, J. Pencer, J. N. Sachs, J. F. Nagle, and J. Katsaras
Langmuir, **23**, 1292 (2007).

[12]M. Rappolt, H. Amenitsch, J., Strancar, C. V. Teixeira, M. Kriechbaum,
G. Pabst, M. Majerowicz, and P. Laggner
Adv. Coll. Int. Sci., **111**, 63 (2004).

[13]R. Caminiti, G. Caracciolo, M. Pisani, and P. Bruni
Chem. Phys. Lett. **409**, 331 (2005).

[14]V. Luzzati, P. Mariani, and H. Delacroix,
Makromol. Chem., Macromol. Symp. **15**, 1 (1988).

[15]G. Pabst, M. Rappolt, H. Amenitsch, and P. Laggner
Phys. Rev. E, **62**, 4000 (2000).

[16]T. J. McIntosh and S. A. Simon
Annu. Rev. Biophys. Biomol. Struct. **23**, 27 (1994).

[17]L. Saiz, and M. L. Klein, J. Chem. Phys., **116**, 3052 (2002).

In situ Formation of Solid-Supported Lipid/DNA Complexes

Daniela Pozzi

Gene therapy, because of its aim to eradicate causes rather than symptoms of diseases, is widely believed to be the therapy of the 21st century. Over the last several years, various viral and nonviral methods for gene delivery have been actively investigated. When mixing aqueous solutions of DNA with a suspension of cationic liposomes, highly condensed self-assembled cationic lipid/DNA complexes, named lipoplexes, are formed with the negative charge carried by the phosphate groups of the DNA neutralized by the cationic lipids.[1] On the other hand, because gene transfection involves the formation of discrete complexes, it is well recognized that the enhancement of transfection efficiencies via cationic lipids require a full understanding of all the possible supramolecular structures of lipoplexes at the molecular and self-assembled levels. Accordingly, accurate structural characterization of lipoplexes should help towards a deeper understanding of the mechanisms of transfection and of the mode by which the structure of cationic liposomes affect the physico-chemical properties and biological activity of the lipoplexes themselves. For gene delivery purposes, multi-lamellar vesicles (MLV) are widely utilized consisting of independent scattering domains each of which is a stack of parallel bilayers with the normals to the bilayers in independent stacks isotropically distributed in space. Such powder-like samples weakly diffract and the intensity rapidly falls off with increasing transfer momentum q. Conversely, solid-supported highly aligned lipid multilayers safeguard spatial information and give more intensity for higher orders of diffraction allowing for more accurate diffraction analyses. The major drawback of measuring oriented samples in humidity chambers has for a long time been the so-called vapour pressure paradox (VPP) whose theoretical background explained why aligned multibilayers hydrated from vapour usually exhibited reduced level of hydration. Recently, Katsaras[2] has demonstrated that VPP originated only from experimental inadequacy and has shown that aligned multibilayers can hydrate to the same extent as liposomes immersed in water. As a result, the field of lipid

bilayers structure research has started to use oriented stacks of bilayers hydrated from vapour as model systems of biological membranes.

Here we extended this approach to the *in situ* formation of solid-supported lipoplexes by using highly aligned stacks of membranes as a template. Kinetic experiments performed both by time-resolved energy dispersive X-ray diffraction (EDXD) and synchrotron small angle X-ray scattering (SAXS) allowed us to resolve the lipid/DNA complex formation *in situ*. Furthermore, we retrieved detailed information about the structure, the degree of order and the orientation of the emerging solid-supported lipoplexes, both dehydrated and fully hydrated from a vapour saturated atmosphere. By orientation, important new insight may be obtained into the structural organization of lipoplexes. For example, the lineshape analysis of high-resolution diffraction peaks from oriented samples is expected to clarify the short-ranged positional cross correlations between the DNA of adjacent layers whereas effects of powder-averaging can cause this cross correlations to vanish and not to be observed in un-oriented samples. Thus, the use of oriented samples, could shed more light into the existence of the theoretically predicted 'new sliding columnar phase' of matter which has been supposed to exist in layered systems composed of weakly coupled 2D smectic lattices. Such biomolecular templatings could also be relevant on the future development of practical device engineering of industrial interest.

The EDXD pattern of DOTAP multibilayers system is displayed in Fig. 1 as a function of perpendicular momentum transfer q_z. Four orders of sharp Bragg peaks (BPs) are recorded indicating a high degree of translational order along the normal to the lipid bilayer (z-direction) and a lamellar periodicity of $d=2\pi/q_{00l}$=48.0 Å. The inset labeled as (a) shows a typical rocking curve at the first BP with a central full width at half maximum (FWHM) of 0.06°. From the diffraction pattern of Fig. 1, we also calculated the electron density profile along the normal to the DOTAP bilayers (Fig. 1, inset b) where the electron denser regions (i.e., the two maxima) correspond to the lipid headgroups while the large central minimum corresponds to the region of the hydrocarbon tails.

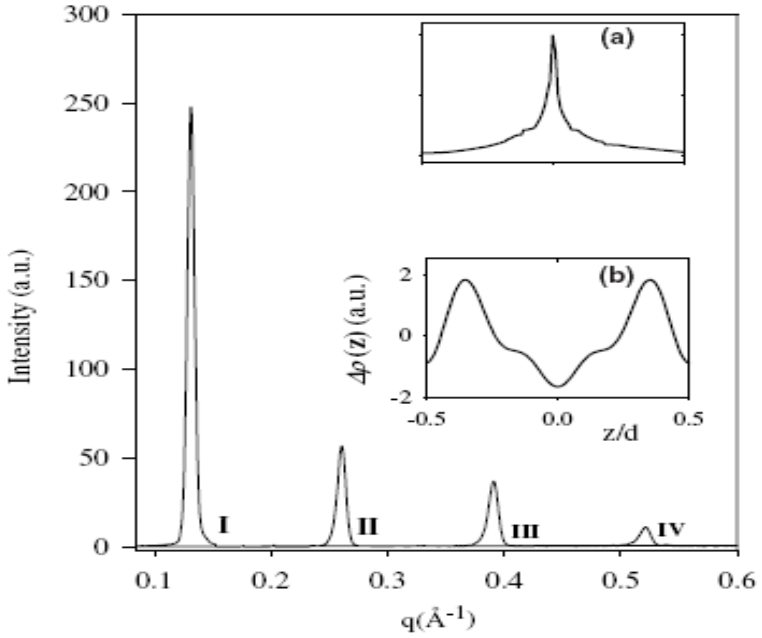

Fig. 1. EDXD pattern of pure DOTAP (T=300 K, RH=50%) shows four sharp Bragg reflections. A representative rocking scan measured at the first Bragg peak (panel (a)) proves the very good alignment of the DOTAP membranes. Electron-density profile along the normal to the bilayers in the L_α phase is also reported (panel (b)).

A drop of 40 μl of a DNA solution 5.6 mg/ml was then carefully spread onto the solid/air interface of the lipid film at a lipid/DNA charge ratio ρ~2, covered the overall surface of the lipid film and the solvent was let evaporate. To resolve the complex formation, time-resolved EDXD patterns were recorded. After the drop spreading, diffraction intensity was accumulated for 100 s per spectrum. In EDXD data collection, no mechanical movement is required, so that the restart of a new spectrum is simply a matter of storing and starting counting again. EDXD patterns representative of the temporal evolution of the system are reported in Fig. 2. To the sake of clarity, the top pattern (t= 0) represents the first-order DOTAP BP immediately before the drop spreading. At t= 50 s (Fig. 2) a single BP is visible at q=0.108 Å^{-1} (d=58.2 Å) which shifts to lower q-values as a function of time up to t= 20000 s (d=63.5 Å). This finding can be interpreted in terms of DNA condensation between opposing DOTAP bilayers. During this period of time, DNA enters the lipid multilayer enlarging the thickness of the interbilayers water regions.

Upon further drying, a progressive shift to higher *q*-values of the BP occurs because the system starts to loose bulk water molecules between opposing bilayers in order to reach the thermodynamic equilibrium with the surrounding environment (relative humidity RH~45%).

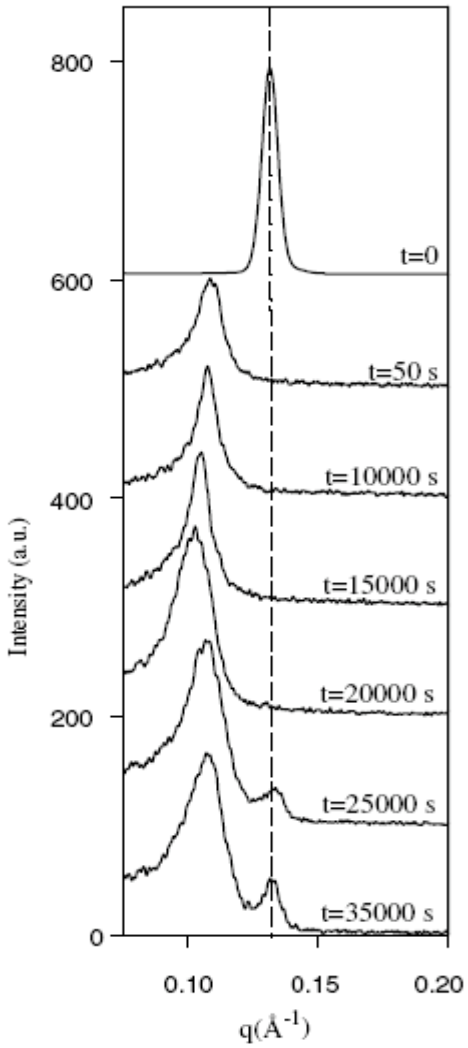

Figure 2. Representative time-resolved EDXD patterns collected upon DOTAP/DNA complex formation as a function of time. The top pattern represents the first-order BP of pure DOTAP before the DNA solution spreading (to clarity intensity was divided by a factor 10). At t=35 000 s, the system is dehydrated and the EDXD pattern shows the presence of predominant DOTAP/DNA complex coexisting with a reduced amount of uncomplexed DOTAP membranes (dashed line).

At t=25000 s, the EDXD pattern clearly shows that the formed DOTAP/DNA complex starts to coexist with uncomplexed original DOTAP membranes as in the case of DOTAP/DNA unoriented lipoplexes.[3] At the final stage (t=35000 s), the pure lipid BP intensity is less than a hundredth of its initial value confirming that the major part of DOTAP membranes is involved in the DOTAP/DNA complex formation. After complete drying, the final EDXD pattern displayed in Fig. 3 (panel a) shows a sharp peak at q=0.113 Å^{-1} corresponding to the (*001*) reflection of an ordered multilamellar structure with a periodicity d=55.7 Å. Our experimental findings are clearly interpretable in terms of DNA condensation between lipid bilayers and are in excellent agreement with structural information previously obtained on unoriented dehydrated lipid/DNA complexes. Therefore, the deposition of the DNA solution immediately resulted in the spontaneous self-assembly of cationic lipids and DNA fragments into the lamellar L_{α}^{C} liquid-crystalline phase. This result has confirmed the general expectation that the physical mechanisms underlying the lipoplex formation are the same even in the case of solid-supported samples, enforcing the idea of using them as model systems for the study of the structural properties of lipoplexes. Before attempting to claim that the proposed experimental procedure effectively resulted in the formation of oriented lipoplexes, the degree of orientation in the samples was promptly investigated. To this end, rocking scans were taken at both the first-order BP of the complex and the lipid and are simultaneously displayed in the inset of Fig. 3 (panel a). The rocking scan proves the good alignment of the lipid/DNA complex with a mosaicity (FWHM=0.1°) lower but comparable with that of the pure lipid system (FWHM=0.06°). The higher FWHM value is due to the onset of stacking disorder induced by the DNA. This is an indication that the DNA fragments intercalate into the aqueous region. between opposing bilayers at the expense of uniformity of alignment. Conversely, the increase of diffuse scattering illustrates the simultaneous presence of liposome-like structures probably induced by hydrophobic interactions at the early stage of the complex formation. While a full discussion on the possible explanations behind this finding cannot be given here, it

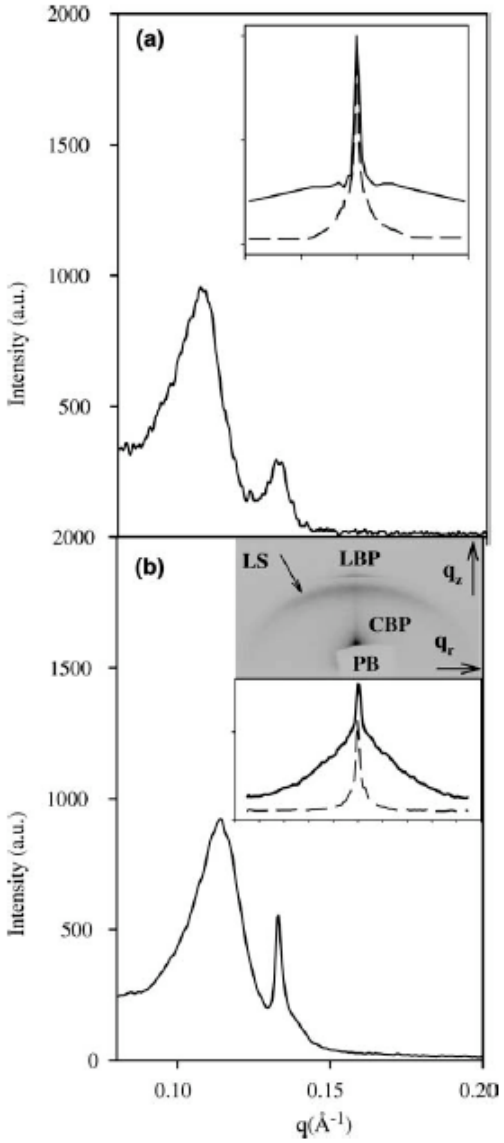

Fig. 3. EDXD pattern of dehydrated DOTAP/DNA complex plus DOTAP membranes (panel (a)). In the inset of panel (a), a direct comparison between the rocking scans measured at the first-order Bragg peak of the complex (solid line) and the pure lipid (dashed line) is reported. In the dehydrated state, the disorder in multilamellar DOTAP structure increases with DNA condensation. In the panel (b), a synchrotron X-ray pattern collected on the same system is shown. In the inset of panel (b), a 2DX-ray pattern (top) elucidates the orientation and of both the complex and the lipid. The first-order Bragg peak of the oriented complex (CBP) and that of the pure lipid (LBP) are evident even if unambiguous traces of liposomes-like structures (LS) are also present. The primary beam (PB) is also indicated. The curves (bottom) obtained by azimuthal integration (complex: solid line; pure lipid: dashed line) strictly confirm the EDXD results.

is only important to note that one can distinguish oriented (prevalent) and unoriented complexes.

In order to shed more light on the degree of orientation of the emerging lipid/DNA complexes synchrotron SAXS measurements were also performed and a representative 2D X-ray pattern is displayed in Fig. 3, panel b. Two evident Bragg reflections, corresponding to *d*-spacings of 57.1 and 48.5 Å, respectively, closely resemble those previously detected by EDXD experiments (Fig. 3, panel a). In addition, 2D X-ray pattern gives unambiguous information about the orientation of the lipoplexes formed *in situ*.

While traces of the first-order BP of the pure lipid (BPL) remain, the SAXS pattern demonstrates that, upon spreading the DNA solution at the lipid/air interface, the DNA fragments penetrate into the major part of the aligned multilamellar DOTAP stacks. Even more remarkably, the pattern indicates that the arising multilamellar structure is preferentially oriented along the *z*-direction. However, subtle Debye–Scherrer rings due to traces of nonoriented liposomal scattering contributions (LS) are also detected. EDXD and SAXS combined results suggest that the overall process can be simply schematized as displayed in Fig. 4.

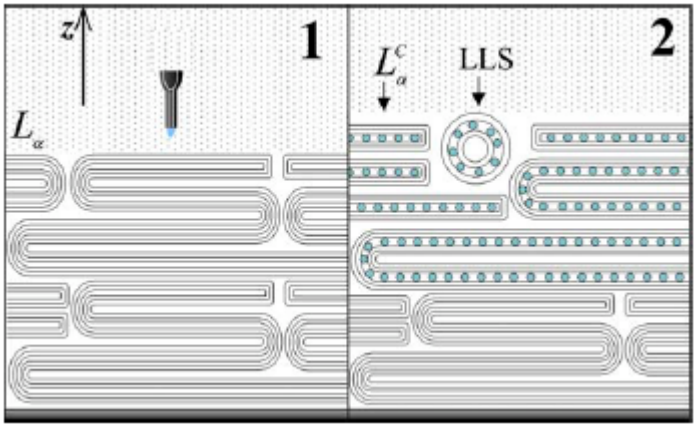

Fig. 4. Solid-supported aligned DOTAP multibilayers system in the liquid crystalline L_α phase (1). A drop of a DNA solution was spread at the lipid/air interface. This resulted in the spontaneous DNA condensation between opposing bilayers, L_α^C phase (2). After excess solvent evaporation, the emerging DOTAP/DNA complex was found to coexist with liposome-likes structures (LLS). The DNA double helices are schematically represented by rods.

The excellent agreement between EDXD and SAXS results confirms that the proposed experimental procedure effectively resulted in the formation of solid-supported DOTAP/DNA complexes preferentially oriented along the normal to the support. The proposed experimental procedure resulted in the formation of solid-supported lipid/DNA complexes with a sensible reduction of the typical EDXD acquisition times. Our combined EDXD and SAXS results confirm that the inner structure of solid-supported complexes formed *in situ* is essentially the same as their counterpart in aqueous solution. As a result, solid-supported lipid/DNA complexes can successfully emerge as an interesting measurement condition in order to retrieve high-resolution structural information. The good degree of alignment obtained makes it also possible to apply advanced scattering techniques with a precise control of parallel and vertical components of the momentum transfer. Finally, the experimental set-up presented here is amenable to kinetic studies, where membrane active biomolecules solved in the excess water phase can interact with the bilayers. Aside from biomedical applications, since the details of the lipid and DNA molecular structure were not considered, we expect solid-supported DOTAP/DNA complexes to represent a model system and our findings to apply to a wide class of self-assemblies formed between several molecular components including proteins and/or peptides and membranes in their liquid-crystalline L_α state.

References

[1] P.L. Felgner, T.R. Gadek, M. Holm, R. Roman, H.W. Chan, M. Wenz, J.P. Northrop, G.M. Ringold, M. Danielsen, Proc. Natl. Acad. Sci. USA 84 (1987) 7413.

[2] J. Katsaras, Biophys. J. 75 (1998) 2157.

[3] G. Caracciolo, R. Caminiti, D. Pozzi, M. Friello, F. Boffi, A. Congiu Castellano, Chem. Phys. Lett. 351 (2002) 222.

SOFT MATTER

1) F. Boffi, R. Caminiti, S. Capuani, A. Giovannelli, C. Sadun, A. Congiu Castellano
A structural and kinetic study by energy dispersion x-ray diffraction: interaction between 1,4-dihydropyridines and biological membranes.
Chem. Phys. Lett., 286(5-6), 473-478 (**1998**).

2) G. Caracciolo, G. Amiconi, L. Bencivenni, G. Boumis, R. Caminiti, E. Finocchiaro, B. Maras, C. Paolinelli and A. Congiu Castellano
Conformational study of proteins by SAXS and EDXD: the case of trypsin and trypsinogen.
Eur. Biophys. J., 2, 33-39 (**2001**).

3) G. Caracciolo, D. Pozzi, R. Caminiti and A. Congiu Castellano
A new approach for the study of cationic lipid-DNA complexes by energy dispersive X-ray diffraction.
Chem. Phys. Lett., 366, 200-204 (**2002**).

4) G. Caracciolo, R. Caminiti, D. Pozzi, M. Friello, F. Boffi and A. Congiu Castellano
Self-assembly of cationic liposomes-DNA complexes: a structural and thermodinamic study by EDXD.
Chem. Phys. Lett., 351, 222-228 (**2002**).

5) G. Caracciolo, D. Pozzi, R. Caminiti and A. Congiu Castellano
The role of the structural properties in the transfection efficiency of DNA-vectors: a study of a new lipid/DNA complex.
Eur. Phys. Journal. E., 10(4), 331-336 (**2003**).

6) G. Caracciolo, M. De Spirito, A. Congiu Castellano, D. Pozzi, G. Amiconi, A. De Pascalis, R. Caminiti and G. Arcovito
Protofibrils within fibrin fibres are packed together in a regular array.
Thromb. Haemostasis, 89, 632-636 (**2003**).

7) G. Caracciolo, G. Mancini, C. Bombelli, P. Luciani and R. Caminiti
The structure of the Gemini surfactants self-assemblies investigated by energy dispersive X-ray diffraction.
J. Phys. Chem. B, 107(44), 12268-12274 (**2003**).

8) G. Caracciolo, C. Sadun and R. Caminiti
Hydration kinetics of oriented lipid membranes investigated by energy dispersive X-ray diffraction.
Appl. Phys. Lett., 85(9), 1630-1632 (**2004**).

9) G. Caracciolo, G. Mancini, C. Bombelli and R. Caminiti.
Structural features of a cationic gemini surfactant at full hydration investigated by EDXD.
Chem. Phys. Lett., 386, 76-82 (**2004**).

10) G. Caracciolo, C. Sadun, R. Caminiti, M. Pisani, P. Bruni, O. Francescangeli
Structure of solid-supported lipid–DNA–metal complexes investigated by energy dispersive X-ray diffraction.
Chem. Phys. Lett., 397(1-3), 138-143 (**2004**).

11) G. Caracciolo, H. Amenitsch, C. Sadun and R. Caminiti
In situ formation of solid-supported lipid/DNA complexes.
Chem. Phys. Lett., 405, 252-257 (**2005**).

12) R. Caminiti, G. Caracciolo and Michela Pisani
Effect of hydration on the structure of oriented lipid membranes investigated by in situ time-resolved Energy Dispersive X-ray Diffraction.
Appl. Phys. Lett., 86, 253902-253904 (**2005**).

13) R. Caminiti, G. Caracciolo, Michela Pisani and Paolo Bruni
The effect of hydration on the long-range order of lipid multilayers investigated by in situ time-resolved Energy Dispersive X-ray Diffraction.
Chem. Phys. Lett., 409, 331-336 (**2005**).

14) G. Caracciolo, S. Piotto, C. Bombelli, R. Caminiti and G. Mancini
Segregation and phase transition in mixed lipid films.
Langmuir, 21(20), 9137-9142 (**2005**).

15) G. Caracciolo, M. Petruccetti and R. Caminiti
A new experimental set up for the study of lipid hydration by Energy Dispersive X-ray Diffraction.
Chem. Phys. Lett., 414, 456-460 (**2005**).

16) M. Pisani, P. Bruni, G. Caracciolo, R. Caminiti and O. Francescangeli
Structure and Phase Behavior of Self-Assembled Dipalmitoylphosphatidylcholine-DNA-Metal-Cation Complexes.
J. Phys. Chem. B, 110(26), 13203-13211 (**2006**).

17) G. Caracciolo, R. Caminiti, A. Martinelli, D. Pozzi, G. Amiconi, G. Boumis and A. Congiu Castellano
Conformational changes of bovine B-trypsin and trypsinogen induced by divalent ions: an energy dispersive x-ray diffraction and functional study.
Arch. Biochem. Biophys., 429(1-2), 157-163 (**2006**).

18) G. Portale, A. Longo, V. Rossi Albertini, L. D'Ilario, A. Martinelli and R. Caminiti
Small-angle energy-dispersive x-ray scattering using a laboratory-based diffractometer with a conventional source.
J Appl. Cryst., (**2007**) .in press

The Energy Dispersive X-ray reflectometry for the study of surfaces and layered media

Valerio Rossi Albertini

The Energy Dispersive X-ray reflectometry technique (EDXR) is a powerful method for investigating monolithic and multilayered film structures. X-ray at grazing incidence studies are highly sensitive to electron density gradients (irrespective of the crystalline or amorphous nature of the system investigated) and allows one to extract information not only on the free surface and the interface(s), but also to determine with great accuracy the mass density, the thickness and the roughness of thin layers along the direction normal to the specimen surface.

A simplified description of the basic principles of the physical phenomenon of total external reflection can be given in term of classical optics, that is the refraction and reflection effects. Measuring the incidence and reflection angles from the surface, the Snell's law for refraction can be written as: $n_1 \cos\alpha_i = n_2 \cos\alpha_r$ (α_i and n_1 being the incidence angle of the primary beam and the refractive index of the first medium and α_r and n_2 the reflection angle and the refractive index of the second medium, see fig. 1).

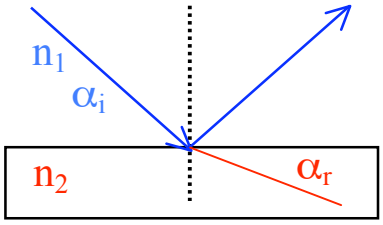

Fig. 1. Schematic sketch of the interaction of an X-ray beam upon a surface.

If $n_1 > n_2$, than $\alpha_i > \alpha_r$. Consequently, there must be a value of α_i, called critical angle α_c, so that $\alpha_r = 0$. In this case $\cos \alpha_c = n_2 / n_1$. If the first medium is air ($n_1 \cong 1$), than the expression becomes: $\cos \alpha_c = n_2$. In these

conditions, the beam will not be refracted any longer but totally reflected. In case of X-ray this optical model still applies, the only change required being a different definition of the refractive index. The (complex) index of refraction in the X-ray region can be indeed written as: $n = 1- \delta-i\beta = 1-(\lambda^2/2\pi)\,\rho\, r_0\, Z^2 - I\ (\lambda/4\pi)\,\mu$, where the real term δ is associated with the dispersion, the imaginary term β with the absorption of X-rays (negligible), λ is the radiation wavelength, ρ is the electron density and r_0 is the classical electron radius. Substituting such expression of n in the previous Snell law for and taking into account that the incident angle is extremely small (so that the function $\cos\alpha$ can be expanded at the third order in Mc Laurin series), we obtain $\alpha_c/\lambda =$ constant. Under the same hypothesis of small angle ($\sin\alpha \approx \alpha$), and since the scattering parameter (momentum transfer) is $q \cong 4\pi\sin\alpha/\lambda$, the X-ray total reflection occurs when the scattering parameter is below a critical value $q_c = 4\pi\alpha_c/\lambda$.

Therefore, at a very good approximation, in a total reflection experiment far from the absorption edge, the relevant parameter is not the critical angle alone, which changes with the X-ray energy, but rather the critical angle to wavelength ratio, i.e. the critical value of the scattering parameter q_c where: $q = 4\pi\sin\alpha/\lambda = K\ E\ \sin\alpha$ (Where E is the energy and the constant K = 1.0136 $Å^{-1}$/keV). Since a reflectivity measurement consists of collecting the reflected intensity as a function of the scattering parameter, two methods are available to perform the q scan and to draw the reflected intensity profile as a function of it: (i) to use a monochromatic beam (fixed Energy), and to make an angular scan, called the Angular Dispersive mode (AD); (ii) utilizing a continuum spectrum radiation (often called *white beam* in analogy with visible light), keeping the scattering angle fixed, referred as Energy Dispersive mode (ED). Advantages and disadvantages [1,2,16] of one method on the other have been fully discussed elsewhere but it is worth to

remarking that the experimental geometry remains unchanged during data collection, which is a fundamental advantage for *in situ* studies, as in this case.

If the sample is a thin film, the primary X-ray beam is partially reflected and partially refracted at its surface (see fig. 2). The refracted component is, in turn, partially reflected at the interface with the substrate, thus moving back towards the surface. When it re-emerges from the film, a new back-refraction deviates it in a direction parallel to the component reflected at the surface.

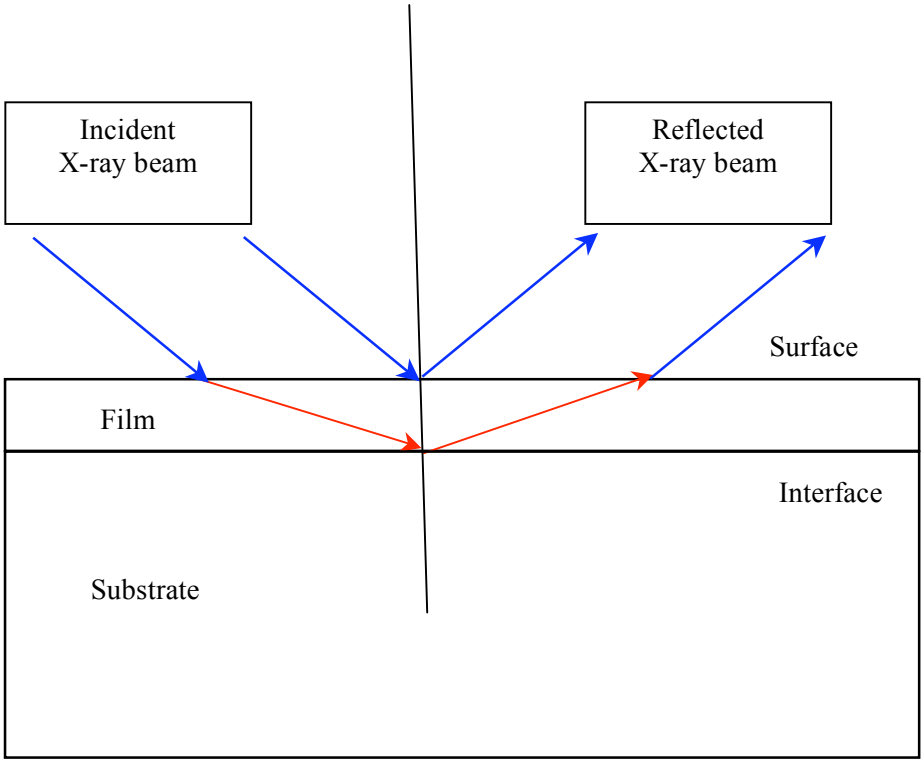

Fig.2. Scheme of the reflection/refraction of the primary X-ray beam at the film surface and interface with the substrate.

However, the component that has travelled along the film bulk is no longer in phase with the component reflected at the surface. As a consequence, the two components interfere and, at a first approximation (according to the Bragg model of semi-reflecting mirrors), the wavelength of the modulation of the interference function Δq will be inversely proportional to the distance between surface and interface, that is to say to the film thickness (see the following experimental section).

In addition, analogously to the Debye-Waller treatment of the thermal displacement of the scattering atoms in diffraction measurements, it turns out that fluctuations in the film thickness will result in an exponential decrease of the interference function.

Therefore, a fit of the reflectivity spectrum provides both the average film thickness (equal to $2\pi/\Delta q$) and the mean squared deviation from such thickness (called roughness) or, in other terms, the first and the second momenta of the local film thickness distribution function.

A more rigorous discussion on the reflectivity measurements and on the information attainable from them, together with the extension to the case of multilayers and superlattices exhibiting multiple interfaces, is contained in the review paper reported in the references.

Energy Dispersive X-Ray Reflectometry as a tool for material science investigation

Amanda Generosi

NO_2 sensing Ruthenium Phthalocyanine devices

The morphologic effects induced by the physical-chemical interactions occurring between $(RuPc)_2$ thin films and NO_2, represented the scientific goals of this work[1,2.] Traditionally gas sensors are studied by optical/conductometric techniques because the result of the interaction with oxidising gases is usually a change in the absorbance spectra or in conductivity. However, neither the gas-sensing process had never been studied in real time, nor the kinetics ruling such process. Energy Dispersive X-ray Reflectometry (EDXR) is a technique able to study morphological characteristics of layered samples, at the A resolution. This was the main tool used to investigate the sensing potential of the $(RuPc)_2$ and to deepen the knowledge of the basic interactions occurring inside the films matrix when they come in contact with the NO_2 gas. EDXR time-resolved in-situ measurements were used to monitor the morphological time evolution of such systems that undergo specific treatments [7,8].

The gas sensing films were grown with thicknesses ranging from 20 nm to 150nm, with a surface area of ≈ 1 cm^2. They were placed in the experimental chamber and exposed to a gas flux of N_2 containing 50 ppm of NO_2 , which corresponds in our setup to a rate of 20 nmol/s. After a complete saturation was reached, each film was submitted to a desorption treatment by flushing the systems with pure N_2 gas at 180 nmol/sec for another day and, finally, the samples were left in air (room conditions) and periodically (every month) re-measured (ex situ EDXR) to check their morphological stability. As an example, two sequences of reflectivity spectra are shown in fig. 1(a), in the case of two films having nominal thicknesses of 50nm and of 100nm, respectively. The real time evolution of the thickness and roughness parameter resulting from the Parratt fitting is reported in detail in fig. 1(b).

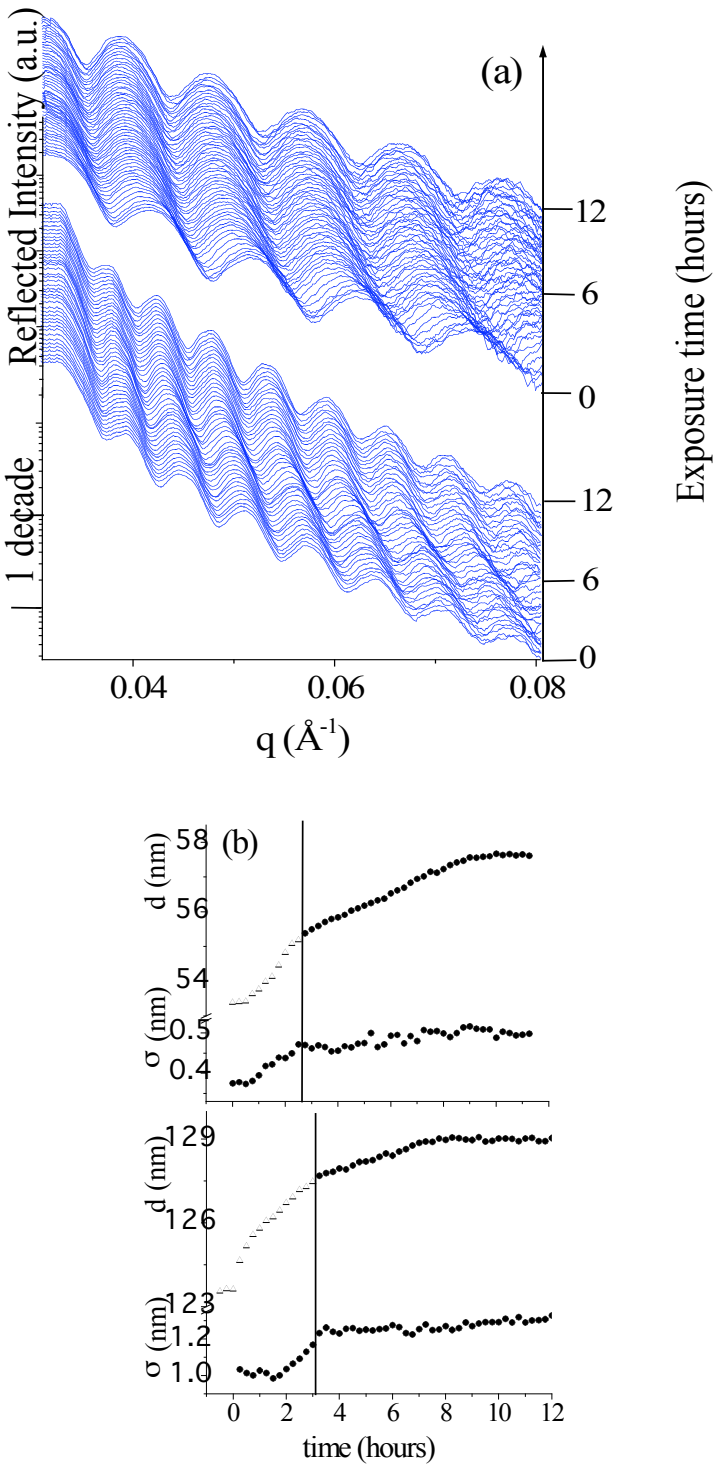

Fig. 1. (a) Reflectivity spectra, collected during the NO_2-film interaction, are plotted as a function of the scattering parameter. (b) The kinetic time evolution of thickness (triangles) and roughness (full dots) is shown. In both examples there is a straightforward correlation between the two-step thickness evolution and the roughness.

In conclusion of a systematic analysis, by time-resolved EDXR, a two-fold reaction mechanism between $(RuPc)_2$ and the active gas resulted evident. A two step process could be inferred [11,17]

The first step, can be related to a surface mechanism with a negligibly small (or no) induction time as enhanced in fig. 1(b) by the straight line; the second, to a diffusion process involving the film bulk. This is consistent with the fact that the packing of the $(RuPc)_2$ thin film is very different from the other MPc, frequently encountered in previous studies [21.]

Photoinduced degradation processes in plastic photovoltaic cells

The electrode-active layer interface of organic photovoltaic (PV) cells, which represents a critical point in the development of organic devices, was studied by EDXR technique applied *in situ*[16]. The results of the real time measurements, performed on different cells upon working conditions, showed that the morphological stability strongly depends on the PV device architecture. The results validate the use of such technique as a powerful tool to provide useful information for the improvement of the devices construction in order to control the fading of their performances [10,18.]

The bulk heterojunction solar cells studied were made from a blend of methano-fullerene [6,6]-phenyl C_{61} butyric acid methylester, denoted PCBM, and MDMO-PPV. The cells consisted of an Indium Tin oxide (ITO) substrate, spin-coated with a 50 nm film of poly(3,4-ethylenedioxythiophene)-poly(styrenesulfonate) PEDOT:PSS (Baytron PH®). An *in situ* experiment was performed on a cell (glass/ ITO/ PEDOT/MDMO-PPV: PCBM/Al) both in the dark and under illumination. In this way any photoinduced modification of the devices morphology can be monitored. The in-situ experiment consisted of collecting a sequence of a large number of X-ray reflection patterns, each acquired for 15 minutes. Each cell under study, (with active surfaces of approximately 0.32 cm^2) was placed in an X-ray transparent chamber, in a controlled atmosphere of N_2 gas flux to prevent contact with external oxidizing agents, and then measured by EDXR as visible in fig. 2 (a). A two step process is evidenced as visible in fig. 2(b). This peculiar behaviour

provides information which establishes the nature of such processes, and supports an hypothesis of electrode oxidation. Indeed, the fact that the interface morphology between the Al electrode and organic material evolves in two steps is consistent with aluminium oxidation kinetics, in which the formation of a passivating layer of alumina is expected to be preceded by the formation of suboxides.

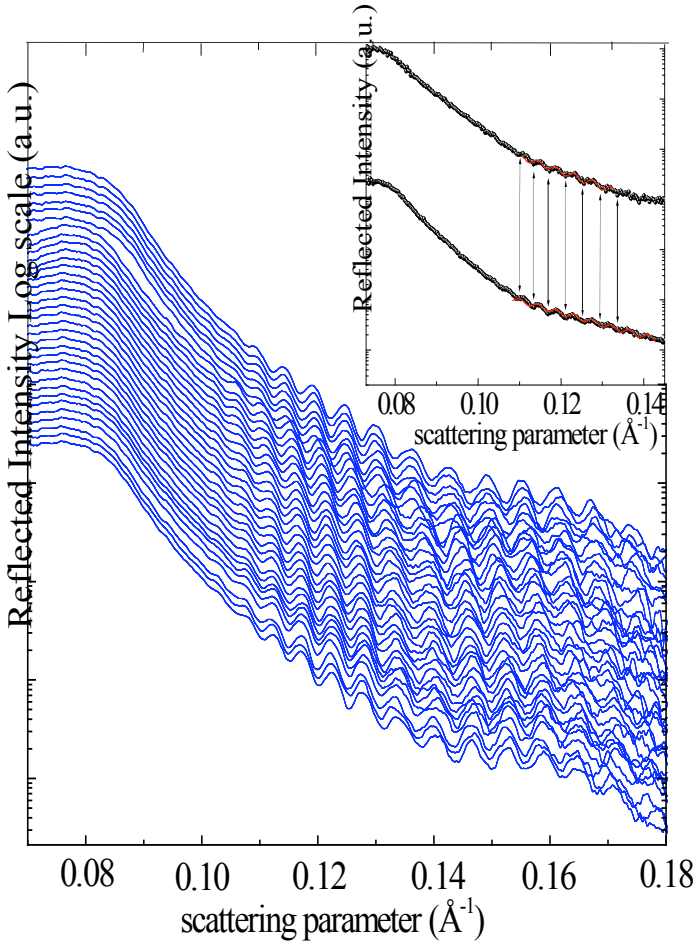

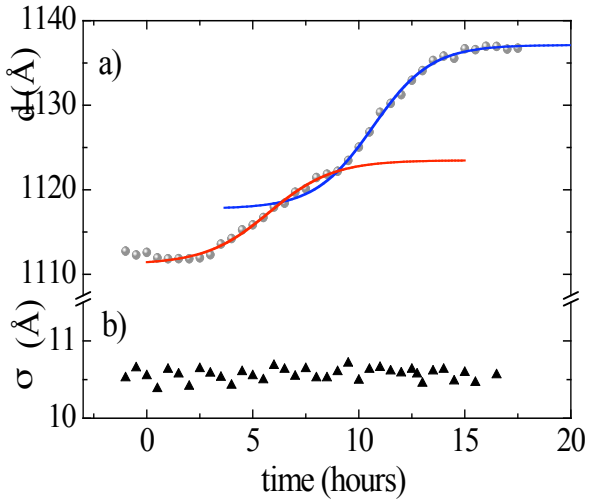

Fig. 2. (a) EDXR measurements of the cell, collected under controlled atmosphere and upon illumination. (b) Thickness and roughness, obtained by fitting the spectra of (a) using Parratt's model, as a function of time. The solid lines represent the fits of the data points by two Boltzman curves.

The morphological data were compared with the efficiency vs time curves measured for the same devices, showing that this process is responsible for a fast reduction of the efficiency of the device. This negative effect was completely inhibited by interposing a buffer layer of LiF between the electrode and the active organic layer in a new sample. The result reported therefore validates the real time morphological monitoring as non standard and very accurate method for retrieving useful information for further improvements in the fabrication of new organic electronic devices.

REFLECTOMETRY

1) A. Generosi, V. Rossi Albertini, G. Rossi, G. Pennesi and R. Caminiti
Energy dispersive x-ray reflectometry of the NO2 interaction with ruthenium phthalocyanine films.
J. Phys. Chem. B, 107(2), 575-579 (**2003**).

2) V. Rossi Albertini, A. Generosi, B. Paci, P. Perfetti, G. Rossi, A. Capobianchi, A.M. Paoletti and R. Caminiti
Time-resolved energy dispersive x-ray reflectometry measurements on ruthenium phthalocyanine gas sensing films.
Appl. Phys. Lett., 82(22), 3868-3870 (**2003**).

3) V. Rossi Albertini, B. Paci, S. Meloni, R. Caminiti and L. Bencivenni
Energy-dispersive X-ray diffraction on thin films and its application to the superconducting samples.
J. Appl. Cryst., 36(1), 43-47 (**2003**).

4) B. Paci, A. Generosi, V. Rossi Albertini, E. Agostinelli and G. Varvaro
Structural, morphological and magnetic study of CoPt/Cr/MgO films EnergyDispersive X-ray Diffractometry and Reflectometry measurements.
J. Magn. Mater., 272-276, 873-874 (**2004**).

5) B. Paci, A. Generosi, V. Rossi Albertini, E. Agostinelli, G. Varvaro and D. Fiorani.
Structural and morphological characterization by Energy Dispersive X-ray Diffractometry and Reflectometry measurements of PLD grown Cr/Pt bilayer films.
Chem. Mater., 16, 292-298 (**2004**).

6) V. Rossi Albertini, B. Paci, A. Generosi, S. Panero, M. A. Navarra and M. di Michiel
In-situ X-ray diffraction studies of the hydration degree of the polymeric membrane in a fuel cell.
Electrochemical and Solid State Letters, 7 (12), 519-521 (**2004**).

7) G. Cicala, P.Bruno, A. Dragone, A. M. Losacco, C. Sadun, A. Generosi
PECVD a-C:H Films for STW Resonant Device
Thin Solid Films, 48, 1-2, 264-269 (**2005**).

8) A. Generosi, B. Paci, V. Rossi Albertini, P. Perfetti, G. Rossi, A. Capobianchi, A.M. Paoletti, G. Pennesi and R. Caminiti
Experimental evidence of a two-step reversible absorption/desorption process in Ruthenium Phtalocyanine gas sensing films by in-situ Energy Dispersive X-ray Reflectometry.
Appl. Phys. Lett., 86, 114106-114109 (**2005**).

9) A. Generosi, B. Paci, V. Rossi Albertini, P. Perfetti, G. Rossi, A.M. Paoletti, G. Pennesi and R. Caminiti
Evidence of a rearrangement of the surface structure in titanium phthalocyanine sensors induced by the interaction with nitrogen oxides molecules
Appl. Phys. Lett., 87, 181904-181907 (**2005**).

10) B. Paci, A. Generosi, V. Rossi Albertini, P. Perfetti, R. de Bettignies, M. Firon, J. Leroy, C. Sentein
In situ Energy Dispersive X- Ray Reflectometry measurements on plastic solar cells upon working.
Appl. Phys. Lett., 87 (1), 194110-194113 (**2005**).

11) A. Generosi, B. Paci, V. Rossi Albertini, P. Perfetti, A.M. Paoletti, G. Pennesi, G. Rossi and R. Caminiti
Morphological variations as non-standard test parameters to determine the sensitivity and the detection limit of gas sensing films : an application to Ruthenium Phthalocyanine.
Appl. Phys. Lett., 88, 104106-104109 (**2006**).

12) A. Generosi, B. Paci, V. Rossi Albertini, P. Perfetti, G. Rossi, A.M. Paoletti, G. Pennesi and R. Caminiti
In-situ Energy Dispersive X-Ray Reflectometry to investigate the (RuPc)2/ NOx interaction process evidenced by ex-situ measurements.
J. Appl. Phys., 99, 1-6 (**2006**).

13) M. Benetti, D. Cannatà, F. Di Pietrantonio, E. Verona and A. Generosi, B. Paci, V. Rossi Albertini
Growth and characterization of highly epitaxial AlN thin films for diamond-based Surface Acoustic Wave devices
Thin Solid Films, 497, 1-2, 304-308 (**2006**).

14) G. Scavia, E. Agostinelli, S. Laureti, G. Varvaro, S. Kaciulis, A. Mezzi, B. Paci, A. Generosi, V. Rossi Albertini
Evolution of the Pt layer deposited on MgO (001) by PLD as a function of the deposition paramenters: a Scanning tunneling microscopy and energy dispersive X-ray diffactrometry/reflectometry study
*J. Phys. Chem. B,*110(11), 5529, (**2006**).

15) P. De Padova, A. Generosi, B. Paci, V. Rossi Albertini, C. Quaresima, B. Olivieri, M. C. Richter, O. Heckmann, F. D'Orazio, F. Lucari, K. Hirkovini
Morphological and magnetic properties of $Ge/Ge_{1-x}Mn_x/Ge$ (001) 2x1 diluted magnetic semiconductor
Surface Science, 900 (18), 4190-4194 (**2006**).

16) V. Rossi Albertini, B. Paci, A. Generosi
The Energy Dispersive X-ray Reflectometry as a unique laboratory tool to investigate morphological properties of layered systems and devices
J. of Phys. D-Appl. Phys., 39, 461-486 (**2006**).

17) L. Alagna, A. Capobianchi, A. M. Paoletti, G. Pennesi, G. Rossi, M. P. Casaletto, A. Generosi, B. Paci, V. Rossi Albertini
The effect of NO_2 on spectroscopic and structural properties of evaporated ruthenium phthalocyanine dimer
Thin Solid Films, 515, 2748-2753 (**2006**).

18) B. Paci, A. Generosi, V. Rossi Albertini, P. Perfetti, R. de Bettignies, M. Firon, J. Leroy, C. Sentein
Controlling photoinduced degradation in plastic photovoltaic cells: a time resolved energy dispersive X-ray reflectometry study"
Appl. Phys. Lett., 89, 043507-043510 (**2006**).

19) E. Agostinelli, S. Laureti, G. Varvaro, A. Generosi, B. Paci, V. Rossi-Albertini, G. Scavia, and A.M. Testa
Study of structural, microstructural and magnetic properties of very thin $Co_{50}Pt_{50}$ films deposited by PLD"
Mat. Sci. Eng. C, Available online 7 September 2006

20) A. Generosi, B. Paci, V. Rossi Albertini, E. Verona, F. Di Pietrantonio, M. Benetti and D. Cannatà.
Structure and morphology of highly epitaxial AlN films for diamond-based Surface Acoustic Wave devices: a systematic study."
Sensors and Actuators A, In Press 2007.

21) P. De Padova, C. Carbone, A. Generosi, B. Paci, V. Rossi Albertini, P. Perfetti, C. Quaresima, B. Olivieri, J. M. Mariot, A. Taleb, I. Berbezier, L. Favre, M.C. Richter, O. Heckmann, F. D'Orazio, F. Lucari, and K. Hricovini
Structural and Magnetic properties of Mn_5Ge_3 nanoclusters dispersed in Mn_xGe_{1-x}/Ge(001)2x1 Diluted magnetic Semiconductors"
Surface Science, In Press 2007.

21) V. Rossi Albertini, B. Paci, A. Generosi, S. Dabagov, O. Mikhin, M. Kumakhov
On the use of Kumakhov Polycapillares to improbe laboratory Energy Dispersive X-ray Diffractometry and reflectometry'.
Spectrochimica Acta B, In Press 2007.

23) A. Generosi, B. Paci, V. Rossi Albertini, P. Perfetti, G. Rossi, A.M. Paoletti, G. Pennesi , R. Caminiti
Real time Joint Energy Dispersive X-ray Reflectivity and conductivity measurements upon NO_2 sensing $Ti(Pc)_2$ devices
Submitted to J. Phys. Chem. B, December 2006

24) B. Paci, A. Generosi, V. Rossi Albertini, P. Perfetti, R. de Bettignies, M. Firon, J. Leroy, C. Sentein
Joint photo-current and morphological monitoring of plastic photovoltaic devices up on working'.
Submitted to Advanced Materials, November 2006

The EDXD technique and the liquid phase: results and perspectives.

Lorenzo Gontrani

The study of the structure of liquid materials is an inherently complex matter, from both a theoretical and an experimental point of view; even the concept of "structure" is hardly applicable to this class of compounds.

As a matter of fact, the strong intermolecular interactions found in solids now turn into weaker attractions that let the molecules (or clusters/supramolecules) explore a very large conformational space, even at low/room temperatures. For this reason, when trying to build a microscopical model of such systems, one cannot help taking into account their "dynamic" character.

From the measure of the intensity of the scattered radiation by the system, its "structure function" *i (q)* can be obtained ("*reciprocal space*"). Through Fourier-transformation of such function, the Radial Distribution Function (RDF) of the sample is deduced ("*direct space*").

This function can be defined as a probability density, (i. e. the ratio of the probability of finding a pair of particles a distance *r* apart, relative to the probability expected for a completely random distribution at the same density), and it is at the basis of the structural interpretation of scattering data. Mathematically, we have:

$$g(r) = \frac{1}{\rho \frac{4}{3}((r+dr)^3 - (r-dr)^3)} \frac{1}{N} \sum_{i=1}^{N} N_j$$

where N_j is the number of particles j such that r-dr<| ri – rj| <r+dr.

The link between g(r) and diffracted intensity for a polyatomic liquid is:

$$4\pi r^2 \sum_m \overline{K_m} \sum_n \overline{K_n} g_n(r) = 4\pi r^2 (\sum_m \overline{K_m})^2 g_0 + \frac{2r}{\pi} (\sum_m \overline{K_m^2}) \int_0^\infty qi(q) \sin rq dq$$

with g_0 is the average density of atoms, *q* is the scattering variable $\frac{4\pi \sin \vartheta}{\lambda}$,

g_n is the distribution for atom type n and K_m is the average effective electron number of atoms of type m. Because of the issues discussed above, the experimental patterns (*I(q)* and the resulting g(r)) obtained from a diffraction

experiment can be attributed to the "mean structure" of the system, corresponding to the equilibrium reciprocal arrangement of its atoms, (provided that the equilibration timescale is not longer than X-Ray measurement time-scale).

From the model structure (possibly more than one, see next), a model structure function can be obtained with the Debye equation for pairs of interaction

$$I_{eu}^{coh}(q) = \sum_{n}\sum_{m} f_m f_n \frac{\sin r_{mn} q}{r_{mn} q}$$

(Note: the summation is usually multiplied by some factor to account for bandwidth: typically, a gaussian of a given standard deviation is used; see next).

I(q) is then transformed to obtain the theoretical RDF; both fuctions are then confronted with experimental curves, thus evaluating the model correctness.The complexity of the model clearly depends on the system conformational mobility, so that, for instance, if a monoatomic liquid or an ionic solution can be described using a limited number of parameters (i. e. water-ion average distances of the first, second (third) coordination shells), polyatomic (non spherical) molecules in solution or neat liquids require that internal degrees of freedom be taken into account. Thanks to the development of simulation methods (Monte-Carlo or Molecular Dynamics) and increase in computational power, sampling of the phase space of complex system has become feasible. Through MD-derived models, we have recently obtained interesting results[5,6]; new papers were submitted or are in preparation.

In these studies, several molecular liquids (pyrrole, furan, tiophene – 2006 – cyclohexane, piperidine and morpholine – 2007) were simulated classically (using different force fields); the trajectory obtained during the MD run was sampled at regular intervals. The snapshots generated constituted as many models, whose structure functions were averaged to obtain a single theoretical function. If the model is obtained in this way, no bandwidth should be imposed, since the sampling itself accounts for thermal uncertainties (peak broadening).

The procedure used is summarized in the following schema:

1) Replication of the molecular structure in 3D to obtain a "pseudo crystal" aggregate(crystal model);

2) Force field/point charges assignement (MMFF94X, GAFF and PEF95SAC were used):

3) Minimization with a given force field (minimized model);

4)MD of the system (droplet) for ~1ns, with coordinate dumping at regular intervals (dynamic model)

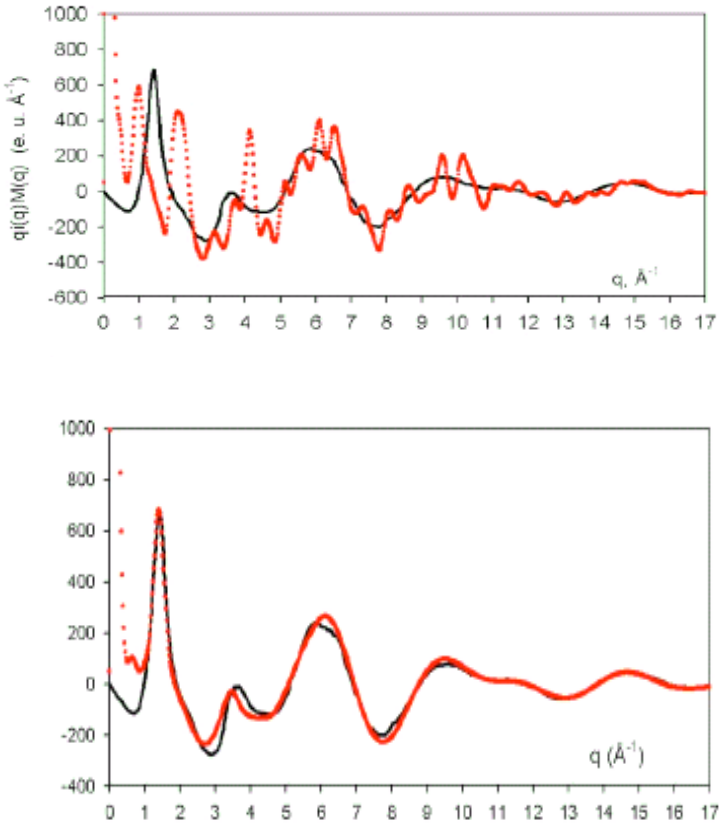

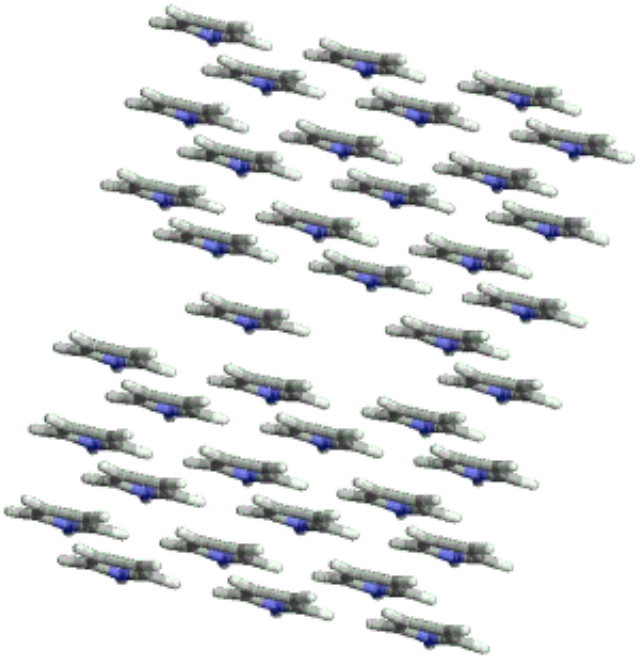

Fig. 4. Starting structure.

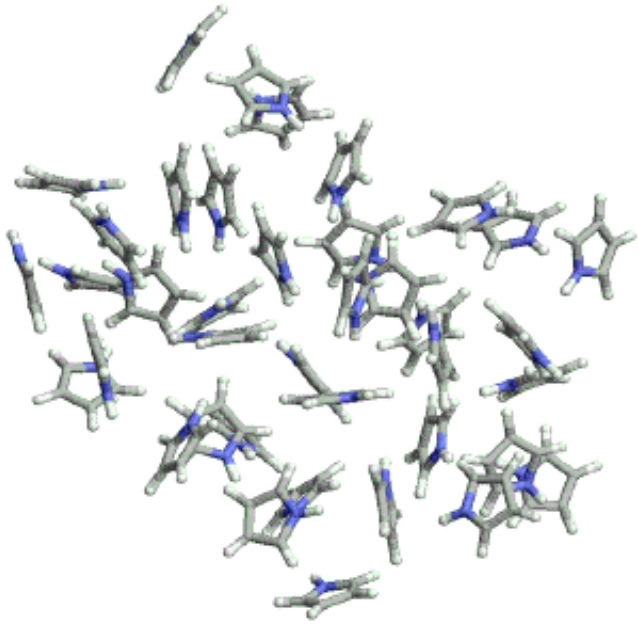

Fig. 5. Average mean structure of MMFF94X trajectory.

Structure functions, radial distribution function and Models of liquid pyrrole [ref 5]

One of the biggest problems of the procedure described is force field choice. While, for instance, the force field MMFF94X (an all atom set developed at Merck) gave very good results for heteroaromatic organic liquids (pyrrole, furan and tiophene), this was not the case of aliphatic liquids (cyclohexane, piperidine and morpholine). General-purpose force fields, in fact, are currently parametrized to reproduce bulk physical observables (i. e. density, heat of formation) or to study biological systems; the parameters contained may not be suitable for molecular liquids.We chose to refine the models by fitting the structure functions to experimental data; in this case, the agreement with experiment was excellent (R Hamilton ~8%). The matter[8] is doubtful, since the benefit of phase space exploration ("dynamic") is lost, and a single model is used.We plan to develop new force fields (RX-oriented) and new simulation strategies. New investigation are currently planned; in particular, a collaboration with a "ionic liquids" research group is likely to start in the next months.

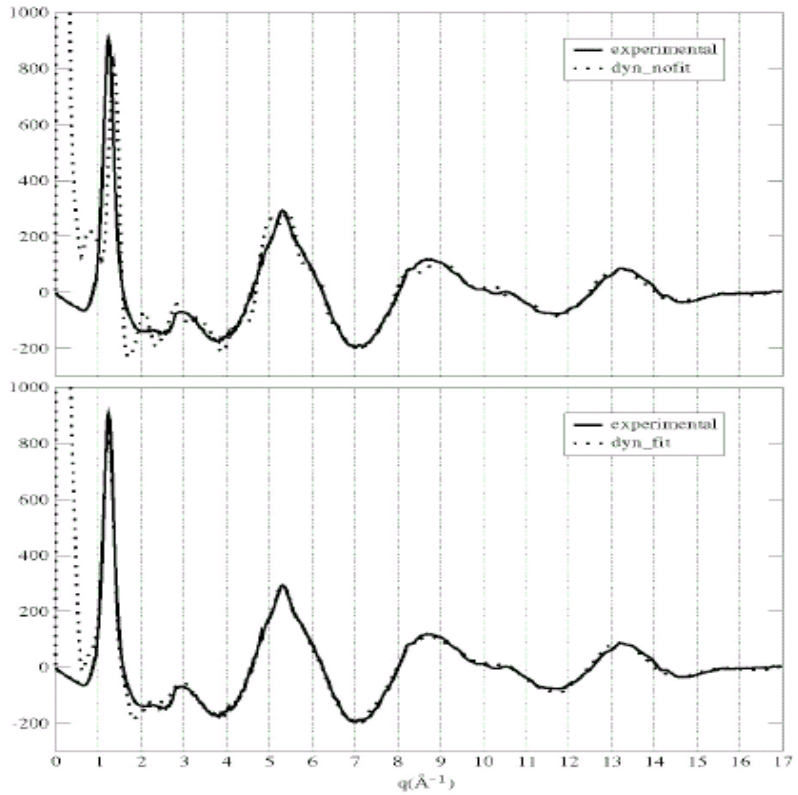

MD structure functions for cyclohexane: fitted and non-fitted.

LIQUIDS AND SOLUTIONS

1) L. Gontrani, R. Caminiti, L. Bencivenni, C. Sadun
Molecular aggregation phenomena in solution: An energy dispersive X-ray diffraction study of imidazole concentrated water solutions.
Chem. Phys. Lett. , 301(1-2) , 131-137 (**1999**).

2) R. Caminiti, M. Carbone , S. Panero, C. Sadun
Conductivity and Structure of Poly(ethylene Glycol) Complexes using energy dispersive X-ray diffraction.
J. Phys. Chem. B, 103(47), 10348-10355 (**1999**).

3) S. Meloni, A. Pieretti, L. Bencivenni, V. Rossi Albertini, C. Sadun , R. Caminiti
SO_2Cl_2, $SOCl_2$: energy dispersive X-ray diffraction, ab initio and molecular dynamics calculation.
Comput. Mat. Science, 20(3-4), 407-415 (**2001**).

4) E. Vasca, G. Palladino, C. Manfredi, C. Fontanella, C. Sadun and R. Caminiti.
An energy dispersive X-ray diffraction study of dioxouranium (VI) in 1 M Lithium citrate.
Eur. J. Inorg. Chem., 13, 2739–2747 (**2004**).

5) L. Gontrani, F. Ramondo and R. Caminiti
Energy dispersive X-ray diffraction and Molecular Dynamics meet: the structure of liquid pyrrole.
Chem. Phys. Lett., 417, 200-205 (**2005**).

6) L. Gontrani, F. Ramondo and R. Caminiti
Furan and Thiophene in liquid phase: an X-ray and molecular dynamics study.
Chem. Phys. Lett., 422, 256-261 (**2006**).

7) M . Di Marco, M . Port, P. Couvreur, C. Dubernet, P. Ballirano, C. Sadun
Structural characterization of Ultrasmall Superparamagnetic Iron Oxide Particles (USPIO) in aqueous suspension by Energy Dispersive X-ray Diffraction (EDXD).
J. Am. Chem. Soc., 128, 10154,10159 (**2006**).

8) L. Gontrani, F. Ramondo and R. Caminiti
Liquid Structure : Theory and Experiment.
J. Amer. Chem. Soc., (**2007**) *Submitted*.

9) M. D'Abramo, R. Caminiti, A. Di Nola and A. Amadei
What can we learn from the comparison among experimental and theoretical-computational X-ray scattering data?
Chem. Phys. Lett., submitted (**2007**)

Supramolecular Organization of Single Nano-Objects by Radial Distribution Function Analysis

Roberto Matassa

Nanostructured materials may be defined as those materials whose structural elements have dimensions in the 1 to 100 nm range, such as: cluster, crystallite or molecules. The explosion in both academic and industrial interest in these materials over the past decade arises from the remarkable electrical, optical and magnetic properties. The link among these properties is the structural characterization of these materials that occur as one progress from an indefinitely extended solid to a particle of material consisting of a *countable number* of atoms. Recently, the structural investigations have extended the study of nano-materials to systems where the nano-objects arise not from the mixture of differently sized particles but from the mixture of particles of different of chemical elements. Using techniques such as x-ray diffraction, long range order and symmetry can be determined by principles such as Bragg's law. The problem is that nano-materials are not periodically long-range ordered and cannot be studied using conventional crystallography (Angular Dispersive X-ray Diffraction ADXD).

In the last decade, the Energy Dispersion X-ray Diffraction E.D.X.D. technique has been subject of several studies to develop new methods of characterization, providing new tools for the materials science. Information about the atomic structure can be gained by experimental measurements of x-ray diffraction. Diffraction patterns produced by sample are obtained by acquiring several measurements by polychromatic source E_{White} at different scattering angles θ_k using the relation $q_k(E_{White}, \theta_k)=\alpha \cdot E_{White} \cdot sin\theta_k$ [$\mathring{A}^{-1}$], defined as *scattering parameters* in the reciprocal space ($\mathring{A}^{-1}$). In order to obtain the overall diffraction pattern, all spectra at fixed q value to different energies must be joined to achieve the experimental static structural function $i(q)$. One merit of the E.D.X.D. compared with the usual one angular dispersion is that the accessible region in the reciprocal space is wider. In the ADXD technique, the maximum q value is limited by the condition $sin\theta \leq 1$, since the source energy is monochromatic. The E.D.X.D. method, once the

scattering angle is fixed, q_{max} is determined by the highest energy component contained in the *white* spectrum. This experimental situation provides an experimental structural function with an overall range from *0.2* to *17.0* $Å^{-1}$ (or from *2.0* to *1.7* nm^{-1}).

On the other hand a drawback must be noticed. Calculating the logarithmic of q: $\Delta q/q = \Delta E/E + cotg\theta\Delta\theta$, we have to take into account that the q resolution decrease with respect to the A.D.X.D. method, in which only the latter term is present. This produces a broad oscillation of the peaks of diffraction pattern yielding the energy dispersive mode particularly suitable for disordered system (amorphous solids, liquids an gases) and not for crystalline samples (Bragg peaks).[22]

In the present short review, we mention recent work on an application of the E.D.X.D. combined with the A.D.X.D. technique, achieving an unequivocal definition of the intra- and intermolecular contacts present in the nano-crystalline material identified as a molecular cluster of dimeric iron phthalocyanines in the solid state.[26] Data by the E.D.X.D. technique were collected in the $2 < q < 170\ nm^{-1}$ range (Fig. 1a), whereas those from the A.D.X.D. technique were obtained in the $2 < q < 40\ nm^{-1}$ range (Fig. 1c). In the common range, the main experimental peaks of the two diffraction patterns are located in the same positions. The Fourier transform of the experimental structural function SF provides the Radial Distribution Function obtained as

$$D(r) = 4\pi r^2\rho_0 + \frac{2r}{\pi}\int_0^{q_{\max}} qi(q)M(q)\sin(qr)dq$$ and reported in the form $D_{iff}(r) = D(r) - 4\pi r^2\rho_0$ in Fig. 1b. The RDF provides direct information in real space on the inter- and intramolecular contacts in the range *0÷5 nm*.

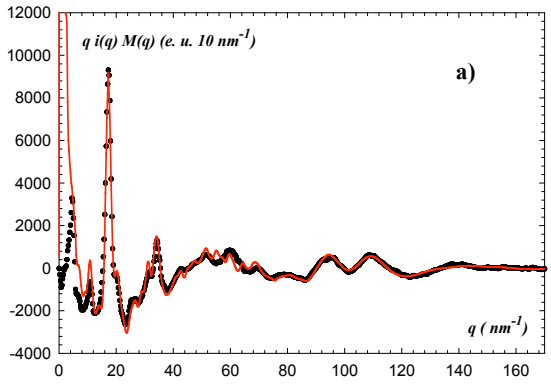

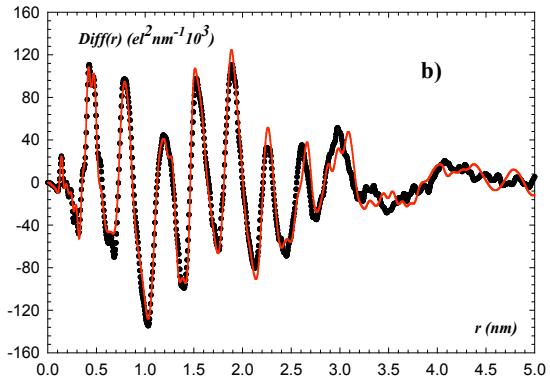

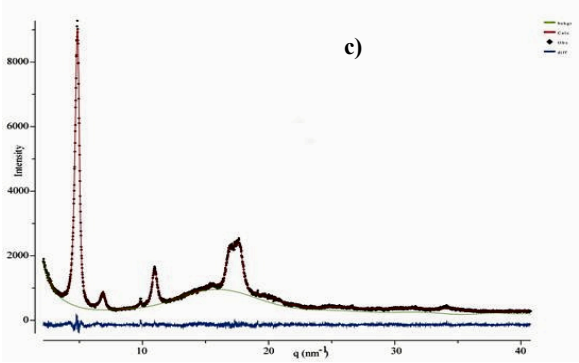

Fig. 1. Structural analysis of the μ-Oxo(2) polymorph by the EDXD technique. **a)** Experimental structural SF (black dots) and theoretical curve (red solid line) calculated for 36 unit cells; **b)** The corresponding Fourier transform *Diff(r)*; and **c)** observed, calculated and difference plots of the Rietveld refinement of the μ-Oxo(2) polymorph of [$(PcFe)_2O$] from ADXD data. Vertical marks refer to the position of calculated Bragg reflections.

Theoretical peak shapes were calculated by Fourier transforming of the theoretical SF, calculated by the Debye equation for the pair interactions of the theoretical models proposed:

$$i_{mn}(q) = \sum_{m \neq n}^{N} f_m(q) f_n(q) \left(\sin(r_{mn} q) / r_{mn} q\right) \exp(-1/2\sigma_{mn}^2 q^2)$$ where r_{mn}

corresponds to the distance between *m* and *n* atoms and σ_{mn} is the root-mean-square (r.m.s.) in the interatomic distance. The ADXD theoretical data was

achieved by the standard Rietveld Program, which was used for refinement of structural parameters (Fig. 1c).

The theoretical RDF analysis has recognized a nano-object constituted of nine dimeric columns of four stacked dimers extended along the *b*- and *c*-axis, having a parallelepiped shape of about 3.5 x 3.5 x 2.6 nm dimension.

In the case the sample show very large experimental peak broadening arising from the lower dimensions of the grains, we present the structural determination of a porphyrin (chiral and achiral) hetero-aggregate by EDXD analysis only.[25] When a chiral structure is imprinted onto an assembly of symmetric molecules by a chiral template or by macroscopic forces (i.e. mechanical effects), through mere non-covalent interactions. The chiral memory phenomenon is of particular interest because, used in combination with the non-covalent strategy, permits to assembly supramolecular species able to perform predetermined functions coupled with chiral discrimination.

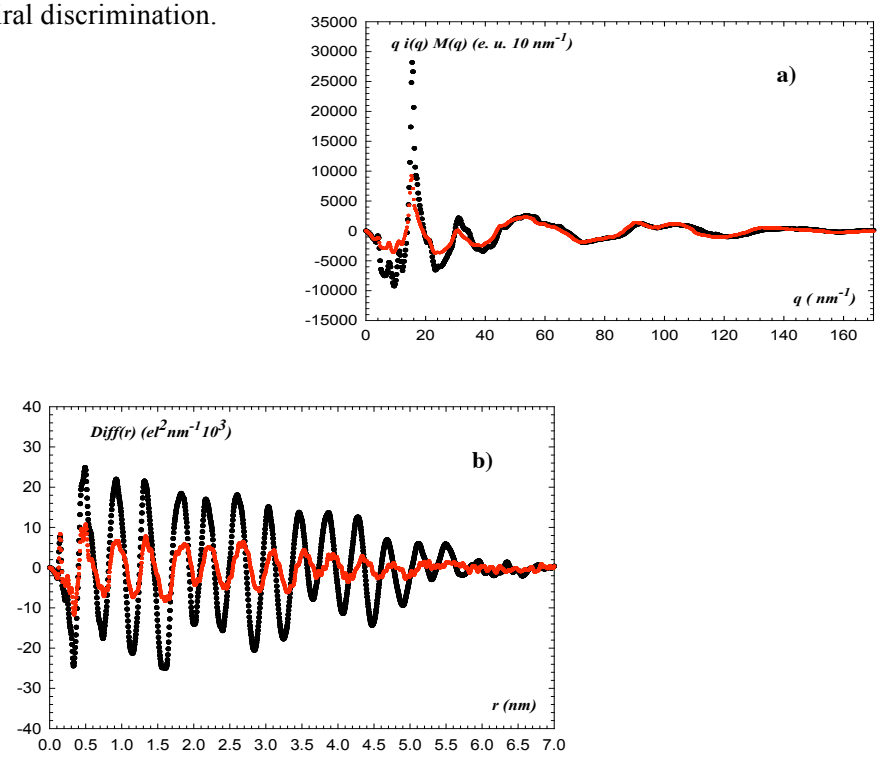

Fig. 2. Experimental X-ray diffraction patterns of the investigated samples:
a) Experimental SF of the imprinted (black dots) and of non-imprinted aggregates (red dots). **b)** Experimental Diff(r)s of imprinted (black dots) and of non-imprinted aggregates (red dots).

The samples were prepared by two porphyrins cationic (CuT4) and anionic (H_2TTPS) hetero-assemblies, one of which was templated with L-phenylalanine and the circular dichroism (CD) was, so far, the only chiral diagnostic tool for hetero aggregates.

The experimental SF's collected in the reciprocal space in the range *2.0* to *170* nm^{-1} show the typical damped oscillations of amorphous samples (Fig. 2a). The intensity of the first two peaks is 3 times lower for the non-imprinted than for the imprinted samples, an indication of a more disordered molecular packing. The Fourier transform of the structure functions yields the radial distribution function *Diff(r)* from *0.1* to *7.0 nm.* The difference of the two samples is even more marked here (Fig. 2b).

The RDF structural analysis of the two samples by EDXD technique shows that the chiral template imprints a suprachiral structure to the porphyrin aggregate. In the suprachiral aggregate the cationic and anionic porphyrins exhibit a *ruffling* distortion and form a dimeric arrangement in an α-helix shape, separated by two different interplanar distances. A model of the template imprinted sample is presented in Fig. 3a. The preparation of the aggregates without inclusion of the template yields an amorphous molecular arrangement, hence an achiral structure (Fig. 3b). Both macrocycles of the hetero-aggregates are characterized by a pronounced distortion of the *saddling* type. The different molecular distortions can be attributed to packing effects in the solid state. The porphyrins in the achiral sample are arranged in a stacking configuration marked by a slipping disorder forming a zig-zag shape, stacked by regular interplanar distance.Finally, we have reported the structural study of materials with a low dimensional molecular aggregation by EDXD technique and RDF analysis. This concerns in particular several advantages: *i)*, more accurate information on the intra- and inter-molecular interaction because of the very extended accessible *q* scattering parameter range; *ii)* allows to spatially probe the different chemical species of the nano-object; and *iii)* determination of supramolecular organization of a single nano-objects by RDF analysis for small volume and/or physical dimensions of nanostructured materials.

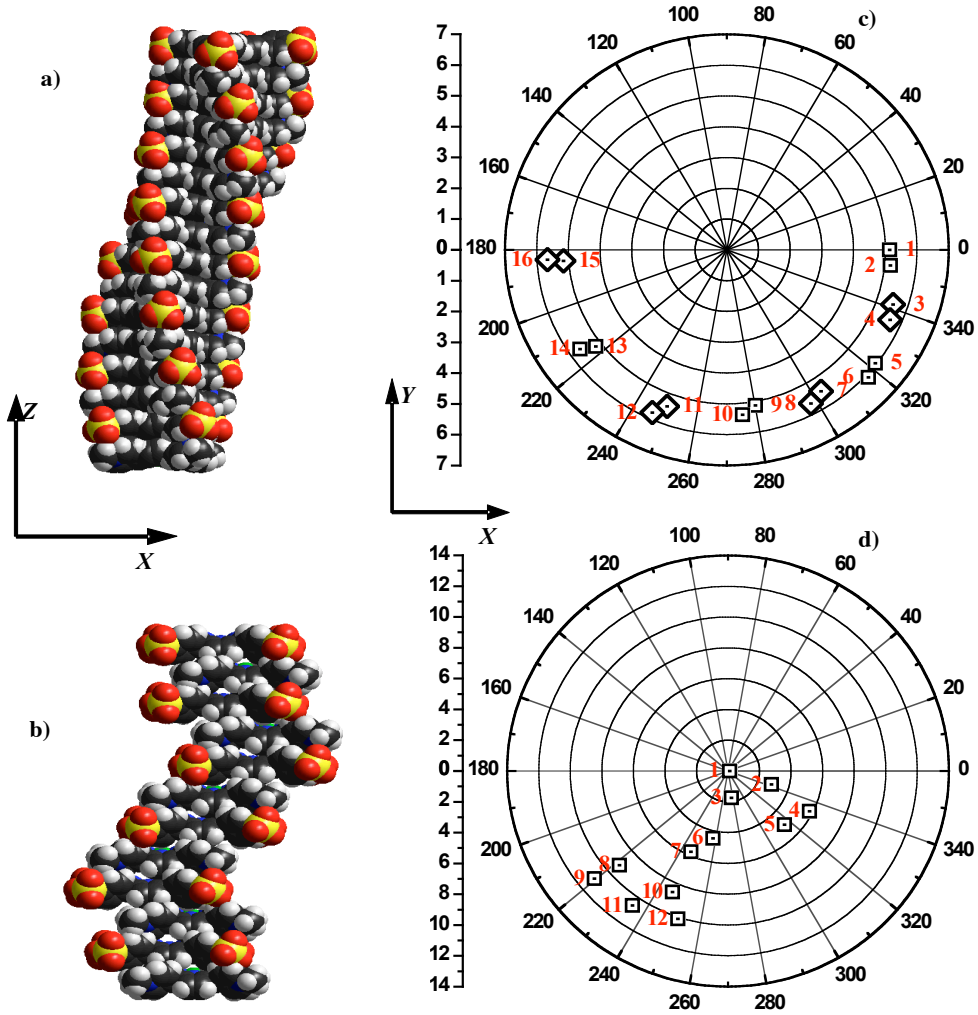

Fig. 3. Three-dimensional molecular packing of the chiral and the achiral samples: **a)** 3D view of the chiral imprinted sample. **b)** 3D view of the achiral non-imprinted sample. Polar plots of the centers of mass viewed from the stack-axis: The stacking axis is perpendicular to the graphic plane and the label numbers increase along the *z*-axis from 1 to N. The initial ray of the polar coordinate system coincides with the positive *x*-axis, and that the ray of 90° coincides with the positive *y*-axis.
c) The imprinted sample shows a dimeric helix aggregation forming approximately one half of a complete turn around the helix axis. **d)** The non-imprinted sample shows a disordered molecular packing, characterized by two clusters of six stack molecules each 180° rotated around the stack axis.

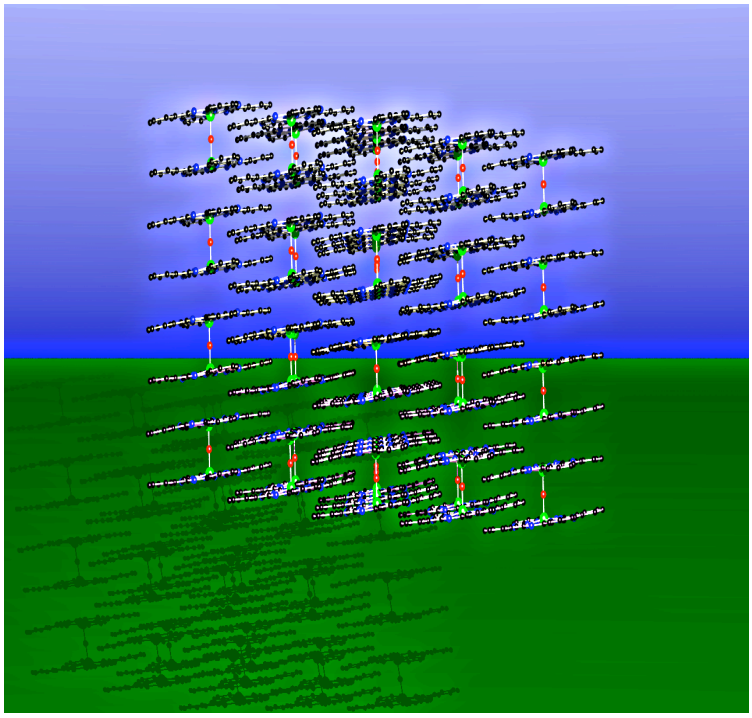

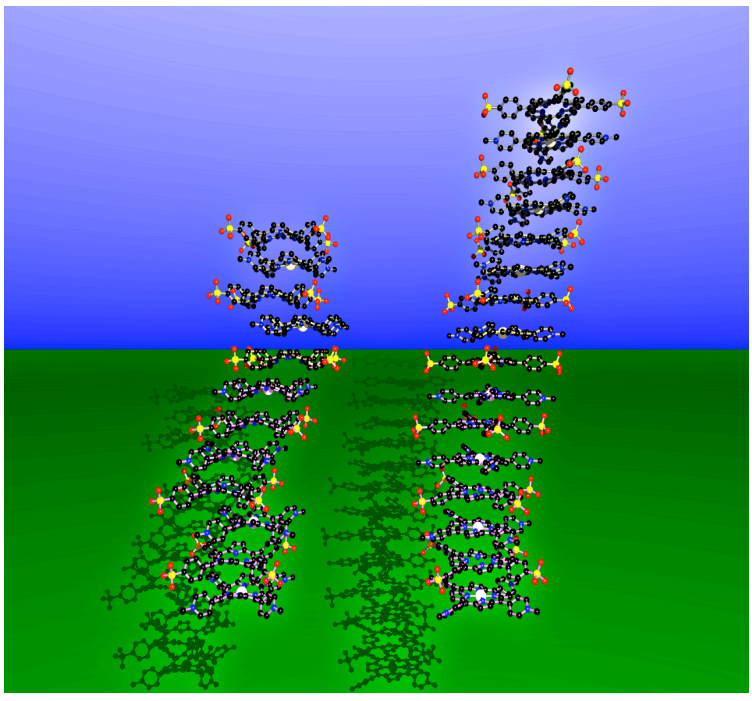

AMORPHOUS AND NANOSTRUCTURED MATERIALS

1) A. Capobianchi, A. M. Paoletti, G. Pennesi, G. Rossi, R. Caminiti and C. Ercolani
Ruthenium Phthalocyanine: Structure, Magnetism, Electrical Conductivity Properties, and Role in Dioxygen Activation and Oxygen Atom Transfer. to 1-Octene.
Inorg. Chem., 33, 4635 (**1994**).

4) D. Atzei, D. De Filippo, A. Rossi, R. Caminiti, C. Sadun
A New amorphous trinuclear complex of PT(II) with 1,3-thiazolidine-2-one: (Pt3(ttz)8)Cl6.
Inorg. Chim. Acta, 248/2, 203 (**1996**).

5) L. Abis, D. Belli Dell'Amico, F. Calderazzo, R. Caminiti, F. Garbassi, S. Ianelli, G. Pelizzi, P. Robino and A. Tomei
N,N-dialkylcarbamato Complexes of Tin as Precursors for the Chemical Implantation of Tin on a Silica Support.
J. of Mol. Catalysis A: Chemica, 108, L113-L117 (**1996**).

6) M. Carbone, R. Caminiti, C. Sadun
Structural Study by energy Dispersive X-ray Diffraction of Amorphous mixed Hydhroxycarbonates containing Co, Cu, Zn, Al.
J. Mat. Chem., 6, 1709-1716 (**1996**).

7) A. Capobianchi, A. M. Paoletti, G. Pennesi, G. Rossi, R. Caminiti , C. Sadun and C. Ercolani
Ruthenium Phthalocyanine and Its Reaction with Dioxygen: Synthesis,Structure, Magnetism and Electrical Conductivity. Properties of the Cofacially Assembled Ruthenoxane Aggregate of formula HO-[(Pc)RuO]n-H (average n=11).
Inorg. Chem., 35, 4643-4648 (**1996**).

8) R. Caminiti, M. Carbone, G. Mancini and C. Sadun
A study of Quaternary Ammonium Tribromide surfactants in solid phase.
J. Mat. Chem., 7(8), 1331-1337 (**1997**).

9) F. Burragato, R. Caminiti, C. Sadun, M. Ferraro, J. Gelli
EDXD-RDF Characterization of maceral group concentrates for assessing coal reactivity.
Fuel, 76(9), 887-892 (**1997**).

10) L. Abis, D. Belli Dell'Amico, C. Busetto, F. Calderazzo, R. Caminiti, C. Ciofi, F. Garbassi and G. Masciarelli
N,N- Dialkylcarbamato complexes as precursores for the chemical implantation of metal cations on a silica support. Part II . Platinum(II) and its further reduction to platinum nanoparticles.
J. Mat. Chem., 8, 751-759 (**1998**).

11) R. Caminiti, M. P. Donzello, C. Ercolani and C. Sadun
Dimeric Osmium Phthalocyanine organized in discrete columnarly stacked Assemblies:structure,magnetism and electrical conductivity properties.
Inorg. Chem., 37, 4210-4213 (**1998**).

12) L. Abis, D. Belli Dell'Amico, C. Busetto, F. Calderazzo, R. Caminiti, F. Garbassi and A. Tomei
N,N- Dialkylcarbamato complexes as precursores for the chemical implantation of metal cations on a silica support. Part III. Palladium(II) and its further reduction to palladium nanoparticles.
J. Mat. Chem., 12, 2855-2863 (**1998**).

13) R. Caminiti, M. P. Donzello, C. Ercolani and C. Sadun
Further Structural Information on the Intra- and Interunit Contacts in Dimeric Ruthenium Phthalocyanine.
Inorg. Chem., 38(13), 3027-3030 (**1999**).

14) D. Atzei, A. Rossi and Claudia Sadun
Synthesis and characterization of a cobalt(III) complex with 1-(D-3-mercapto- 2- methylpropionil)-L-proline
Spectrochim. Acta A, 56, 1875-1886 (**2000**).

16) D. Atzei, T. Ferri, C. Sadun, P. Sangiorgio, R. Caminiti
Structural Characterisation of Complexes between Iminodiacetate Blocked on Styrene-Divinylbenzene Matrix (Chelex100 resin) and Fe(III), Cr(III), Zn(II) in Solid Phase by Energy Dispersive x-ray Diffraction.
J. Amer. Chem. Soc., 123(11), 2552-2558 (**2001**).

17) R. Caminiti, A. Capobianchi, P. Marovino, A. M. Paoletti, G. Padeletti, G. Pennesi, G. Rossi
Structural and Morphological Characterisation of Ruthenium Phthalocyanine Films by EDXD and Atomic Force Microscopy (A.F.M.).
Thin Solid Films, 382, 74-80 (**2001**).

18) R. Saladino, V. Neri, R. Pelliccia, R. Caminiti and C. Sadun
Preparation and structural characterization of polymer-supported methylrhenium trioxide system as efficient and selective catalys for the epoxidation of olefins.
J. Org. Chem., 67, 1323-1332 (**2002**).

19) A. Isopo, C. Tengroth, J. Swenson and L. Borjesson
Structure of Ca0.4K0.6(NO3)1.4 from the glass to the liquid state.
Phys. Rev. B, 64(22), 2242071-2242079 (**2002**).

20) R. Bucci, A. L. Magrì and C. Sadun
Structural Analysis of the Solid Amorphous Binuclear Complexes of Iron(III) and Aluminum(III) with Chromium(III)-DTPA Chelator Using Energy Dispersive X-ray Diffraction.
J. Am. Chem. Soc., 124(12), 3036-3041 (**2002**).

21) R. Matassa, E. Cervone and C. Sadun
Synthesis and structure of amorphous phase Cr(II) hemiporphyrazine using energy dispersive X-ray diffraction.
J. Porphyr. Phthaloc., 7(8), 579-584 (**2003**).

22) M. Carbone, R. Caminiti and C. Sadun
A Review on Energy Dispersive X-ray Diffraction Technique Applied to Disordered Systems.
Research Trends in Chem. Phys., 75-117 (**2005**).

23) Roberto Matassa, Claudia Sadun, Lucio D'Ilario, Andrea Martinelli and R. Caminiti
Supramolecular Organization of Toluidine Blue dye in Solid Amorphous Phases.
J. Phys. Chem. B, (**2007**) . web *3/2/2007*

24) R. Matassa, M. Carbone, R. Purrello, L. Lauceri and R. Caminiti
Supramolecular Structure of Extrinsically Chiral Porphyrin Hetero-Assemblies and Achiral Analogues.
Adv. Mat., (**2007**) . *in press*

25) R. Matassa, C. Sadun, C. Ercolani, M.P. Donzello, P. Ballirano and R. Caminiti
A Nanostructured Polymorph of mu-Oxobis(phthalocyaninatoiron(III)) Studied by angular and Energy Dispersive X-ray Diffraction Techniques.
Nano (**2007**) *in press*.

Compared Edxd-Dsc Studies Of Poly(Ethilene-Succinate) Multiple Melting

Rossi Albertini Valerio

In recent years, polymers have been studied to be employed in new fields (for example as conductive materials ad optical devices), far away from the traditional applications. Important efforts are in progress to develop new experimental techniques or methods to satisfy the increasing request of scientific information on these systems. In particular new methods for studying polymer under variable thermodynamic conditions may be a tool of general interest. Among these, the energy dispersive X-ray diffraction(EDXD) offers an effective and self-sufficient method to face polymeric phase transitions and the general problem of the properties dependence of polymers from temperature. The effectiveness of this method relies on the possibility of exploring the reciprocal space by an X-ray polychromatic beam. Instead of a monochromatic one used in the traditional diffraction technique. In this case the beam is the bremmstrahlung spectrum of a conventional X-ray tube with W anode working at 45 k X-ray tube with W anode working at 45 k X-ray tube with W anode working at 45 kV and 35 mA.

The reciprocal space is sampled electronically instead of mechanically and the experimental procedure becomes simpler because: points of the interference function are acquired simultaneously, though in a limited range of the q-space. Measurements occur at fixed geometry allowing installation of accessory device as pressure

and/ or temperature cell. This work is devoted to investigate the multiple melting phenomena in polymers and to demonstrate the EDXD capabilities complement the standard DSC/DTA analyses usually employed for the comprehension of polymeric thermal behaviour.

2 – EDXD APPIED TO PHASE TRANSITION

Since a long time DSC/DTA has beem the principal mean by which phase transition are investigated. In the rest of this section we briefly illustrate how the

new EDXD method is applied to this kind of problems.For the sake of simplicity the study of a phase transition can be performed following the behaviour of a time dependent variable x(t) equivalent to the reaction coordinate for chemical Process. It may be related to the evolution of the system at the time t with boundary condition

$x(t=0) = 0$ and $x(t= \infty) =1$: in the sense that the system initially in the phase 1, evolves towards the phase 2 (by a transition rate dx(t)/dt).

In the usual EDXD measurements, the structure-sensitive interference function is obtained from the detected intensity through a difficult data processing instead, when EDXD is applied to phase transitions, the problems arising from data correction are overcome. In fact it can be show that x(t), defined as the amount of sample that has turned at the instant t to the final phase ,can be expressed as

$x(t)=[I(t)-I1] /[I2 –I1]$

Since the detected intensity *I*(t) depends on I(t) through multiplicative or additive quantities that do not change during the transition x(t) can be calculated straightforwardly using the observed intensity with no need of processing.

3 –EXPERIMENTAL MEASUREMENTS

3.1) Differential Scanning Calorimetry

A conventional DSC-7 Perkin –Elmer calorimeter was used to perform the termal investigation. Different kind of measurements cycles were carried out in order to check the influence of the crystallisation temperature and of the heating rate on the thermogram profile. Experimental conditions were suitably chosen, in order to make the comparison with EDXD measurements.

3.2) Energy Dispersive X-ray Diffraction

In this work measurements are performed at a fixed scattering angle $\Theta= 3.5°$, the accessible range temperature cell is 20-250 °C, and the detecting system of the diffractometer has been set up to automatically collect and store X-ray spectra of the radiation scattered by the sample while its temperature was increased at the heating rate of 1°C/min. The temperature is measured by a thermocouple inserted

in the sample. The result is a sequence of about a hundred spectra describing the system evolution from 20 °C and increased by 1 °C/min (Fig. 1A, 1B). It is like a movie whose photograms are snapshots taken in the reciprocal space of the evolving system submitted to heating.

The x(t) curve was calculated by following the transformation of the peaks in the (1.3-1.6) $Å^{-1}$, which corresponds to structural changes in the distance range of about (4-5) Å.

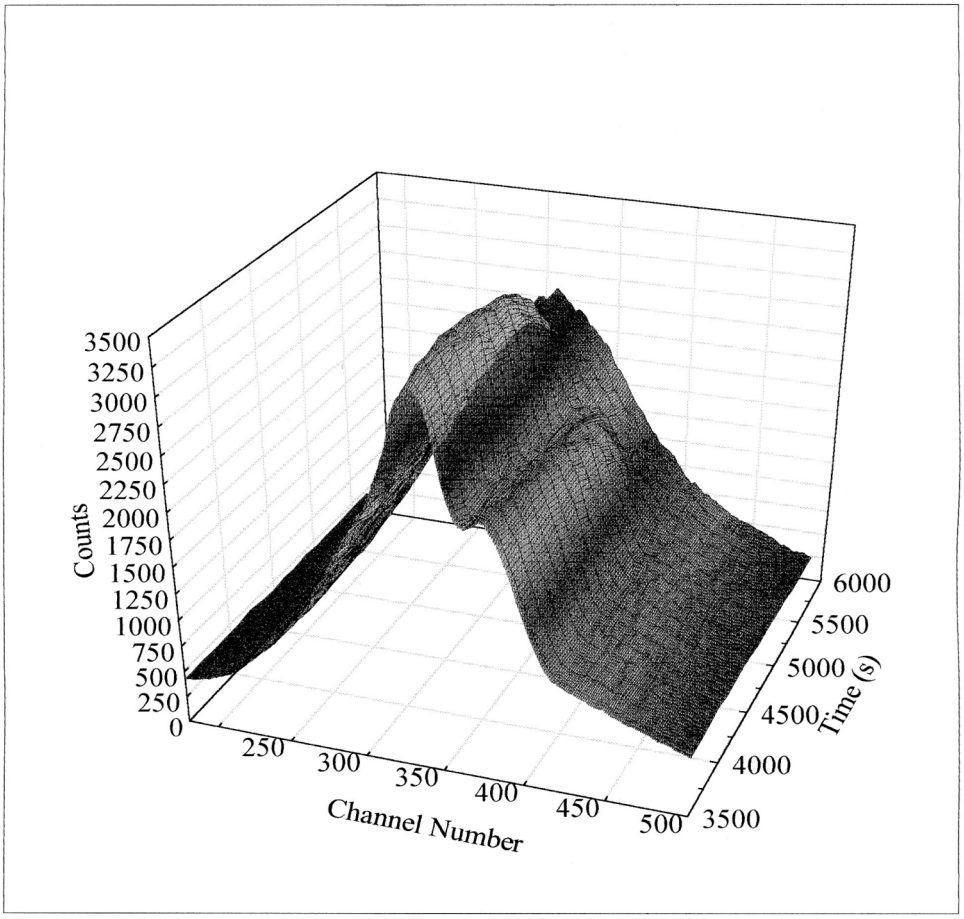

Fig. 1A 3D Plot of the time evolution of EDXD spectra collected during heating of a sample crystallised at T_c= 57 °C

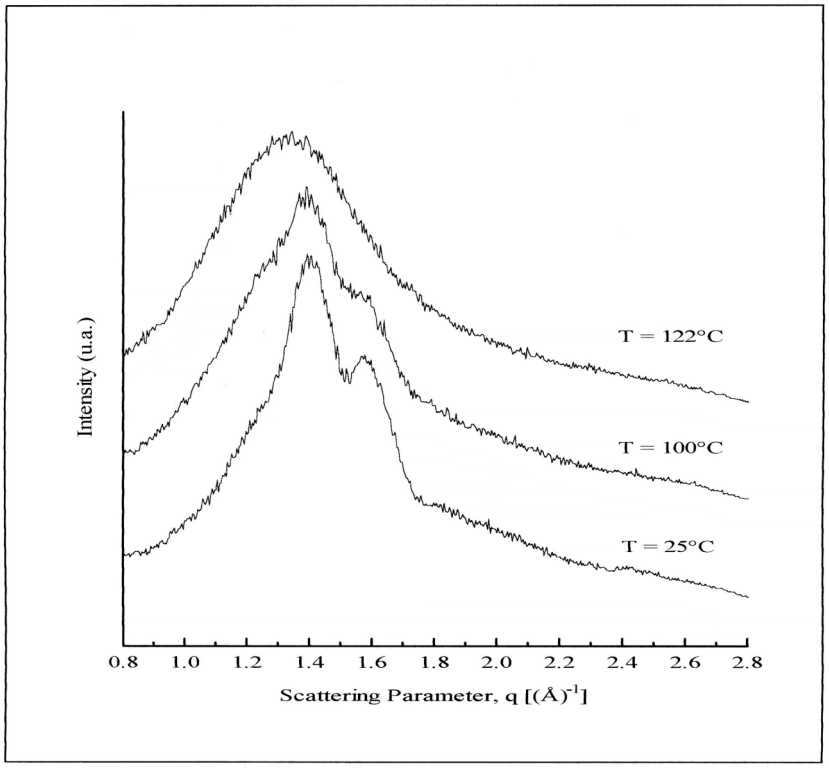

Fig. 1B Selection of the most significative spectra, collected at the key transition points, of the same sample of fig. 1A. The x-axis is now expressed in q-units. Each spectrum is shifted along the y-axis by 1000 units with respect to the previous one. The spectra are labelled by their collection temperatures (heating rate 1 °C/min)

4 – RESULTS AND DISCUSSION

4.1 DSC Measurements

Supposed to be the behaviour of a semicrystalline polymer during melting is determined by its

lamellar structure which, in turn, depends on the thermodynamics and the kinetic conditions of crystallisation. In particular strong dependence on the crystallisation temperature Tc is expected, since it is related to kinetic rate. The sequence of DSC thermogram obtained after melting the sample crystallised at various Tc is shown in Fig. 2.

For the sake of simplicity are shown only thermograms taken at the heating rate of 1 °C/min even is measurements at the heating rates of 10 °C/min and 0.5 °C/min have been performed too.

Peak analysis of DSC spectra, both concerning the position and the intensity, is plotted in Figs. 3, 4A,4B.

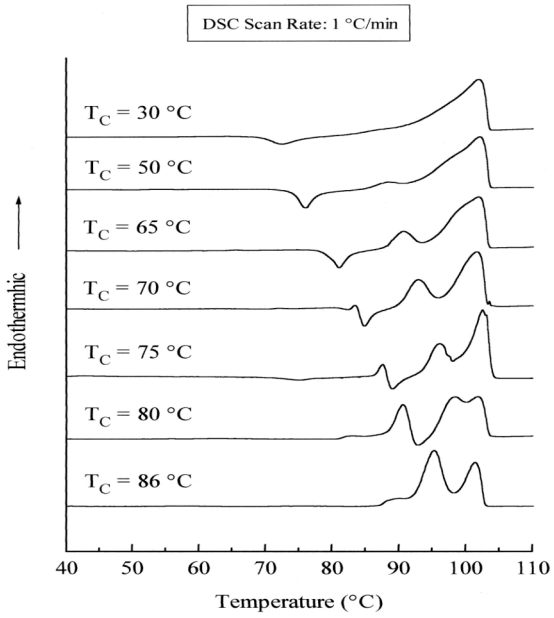

Fig.2 Sequence of DSC spectra taken at the heating rate of 1 °C/min, after crystallisation at the indicated Tc temperatures

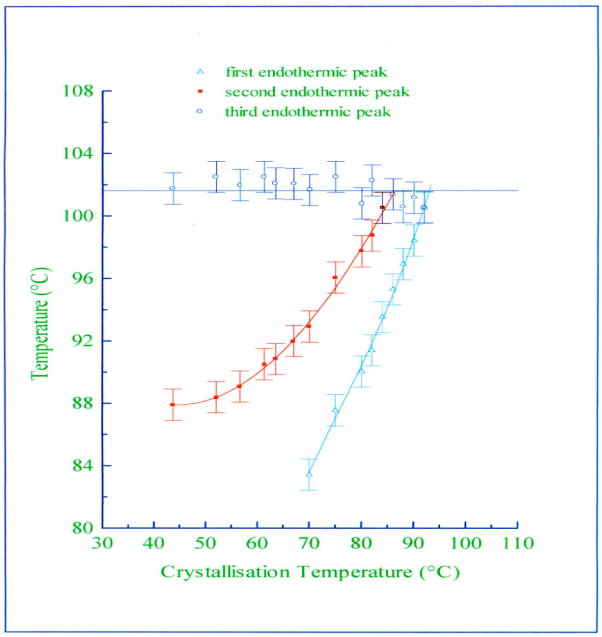

Fig. 3 Temperature positions of endothermic peaks vs crystallisation temperature.

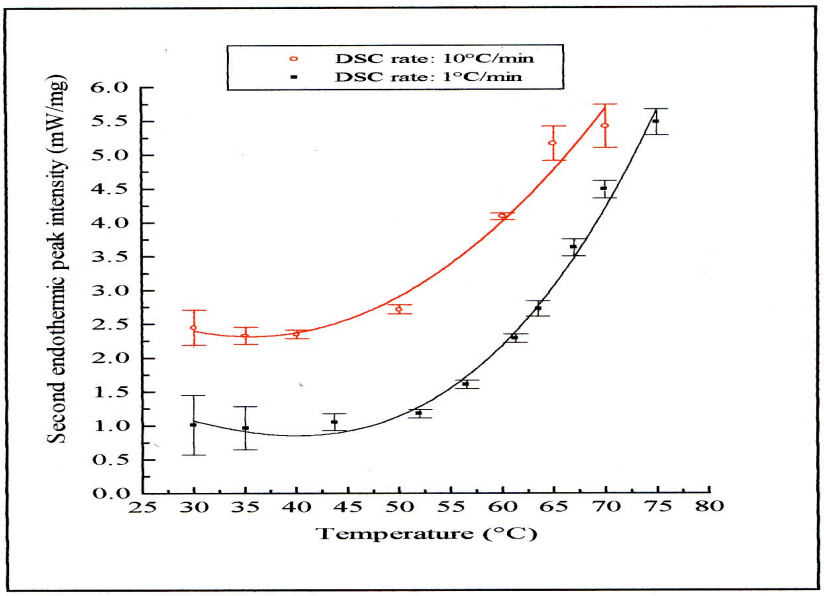

Fig. 4A Intensities of the second endothermic peak vs. T_c fitted by a third order polynomial

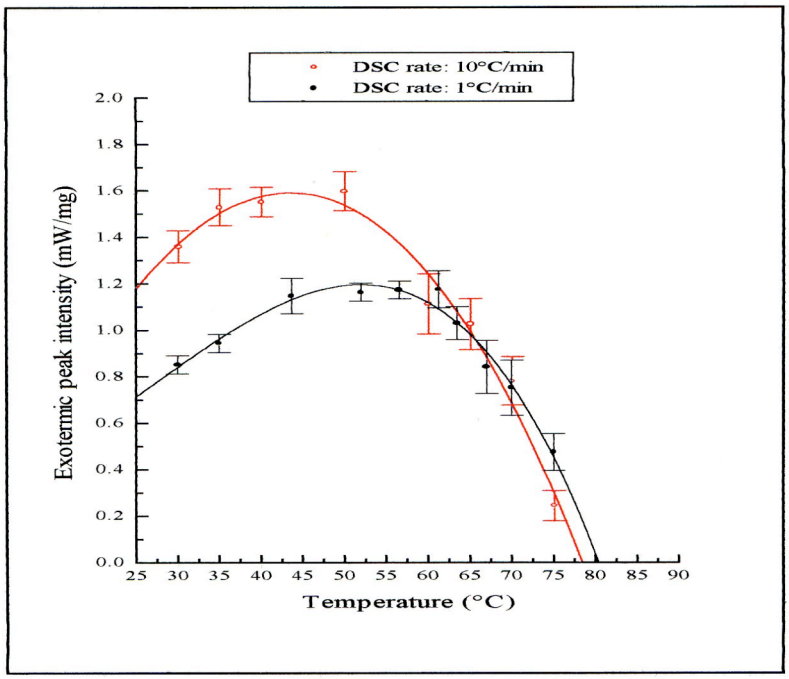

Fig. 4B Intensity of the exothermic peak vs. T_c fitted by a third order polynomial

The aim of this test is to gain information to have indications on which part and what amount of the crystalline structure is undergoing the phase transition and, consequently hypothesise a suitable model for the multiple melting phenomenon in polymers. However, a more straightforward method would consist of using a structure-sensitive probe, like X-ray diffraction to perform the same analysis. In the next section we demonstrate the equivalence of the two approaches.

4.2 EDXD Measurements

In Fig 5 (after sample crystallisation at Tc=61 °C) and in Fig. 6 (after sample crystallisation at various Tc) we show the derivative of x(t) gives a plot analogous to the DSC thermogram. What follow is a qualitative explanation, a more precise mathematical model is being developed.

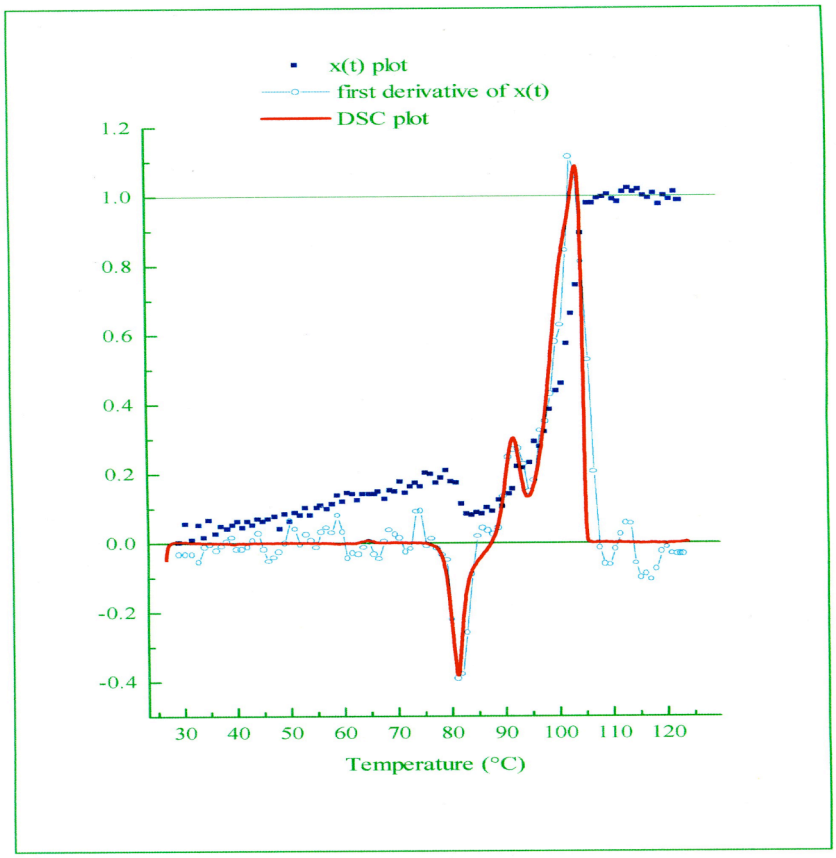

Fig. 5 x(t) plot, obtained from EDXD measurements vs. Temperature, and its first derivative compared with the corrispondent DSC plot. Numerical values on y-axis are referred to x(t). The sample was crystallised at 61 °C.

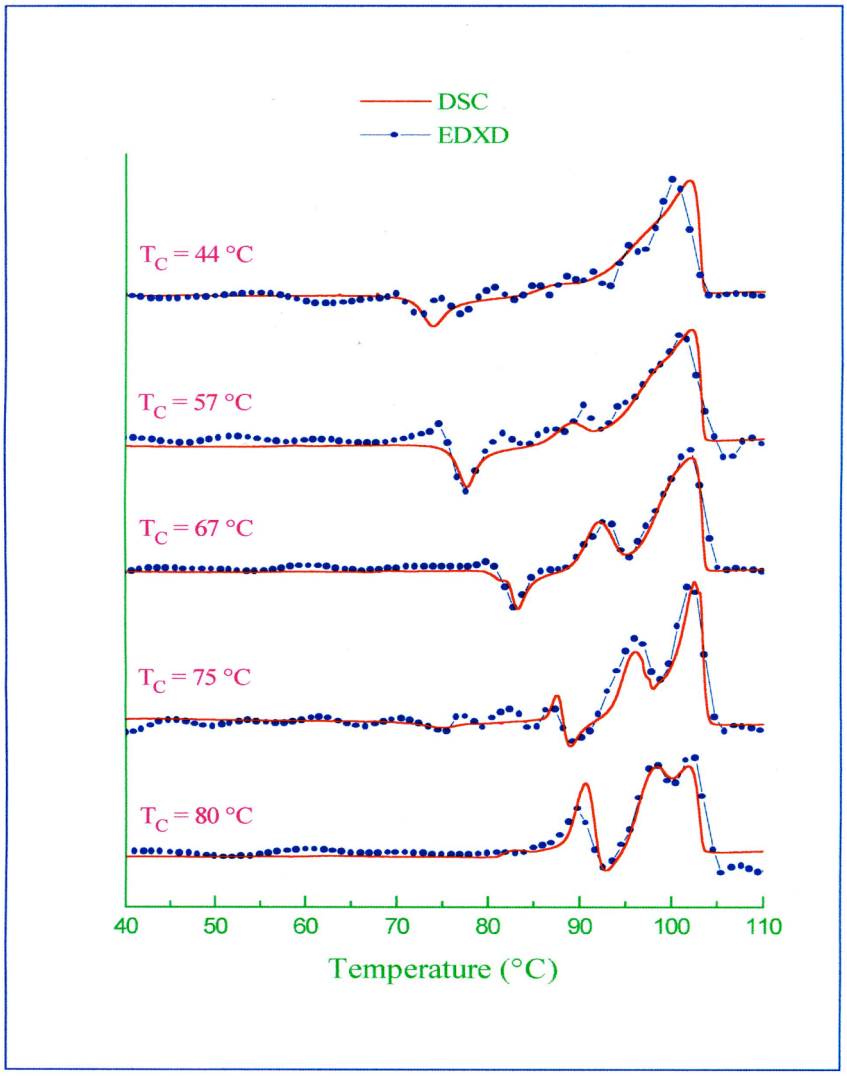

Fig. 6 Comparison between DSC thermograms and first derivative of x(t) for various choices of T_c

A DSC thermogram represents the rate of enthalpy transfer between the system and the environment during a transition and, in costant pressure transformations, enthalpy and entropy are proportional. Now, according to the expression of entropy in the statistical ensemble, entropy can be expressed in terms of the radial distribution function g(r). The most relevant contribution to the latter, in turn, is proportional to the Fourier Transform of S(q) that is contained in the diffraction patterns used to get x(t). Therefore, this is the link: once the time evolution of the

structure dependent quantity x(t) is observed by X-ray diffraction, his first derivative must behave as the heat transfer rate represented by DSC thermogram.

5- CONCLUSIONS

The presence of many peaks in the curve profiles indicates the complexity in the solid state of polymers when variouscrystalline structures coexist, in violation of the phase rule. Melting of each structure produces local maximum in the dx(t)/dt curve, while the single minimum is related to temporary re-crystallisation phenomena i.e. a positive heat transfer in DSC connected to a departure from the final melting state.

The agreement betwween DSC and EDXD measurements means we have a structure sensitive probe whose results may be a complementary source of information on polymeric phase transitionand, possibly, an overcoming of the intrinsic limitations in the former. Moreover, it has been demonstrated the simple model used to describe two-state transitions is good to describe multi-transitions phenomena as well. Improvements are likely to be expected by optimising the experimental conditions and by using a brighter source of X-ray. EDXD seems to be a convenient way to check if the behaviour of this kind of systems is even more complex that that observable by traditional calorimetric methods and, therefore, if new models of polymer transitions should be devised to interpret the experimental evidences.

References 1), 2), 5), 8), 9), 10), 11)

P. Cebe and S.D. Hong Polymer 27,1183 (**1986**)

I.A. Al-Raheil and A.M.A. Qudah Polymer International 37 249 **1995**

K. Konnecke J. Macromol. Sci. Phys. B33(1), 37 **1994**

PHASE TRANSITIONS

1) V. Rossi Albertini, L. Bencivenni, R. Caminiti, F. Cilloco, C. Sadun
A new Technique for the Study of Phase Transitions by Means of Energy Dispersive X-ray Diffraction. Application to Polymeric Samples.
J. Macromol. Sci. Phys. B, 35(2), 199-213 (**1996**).

2) V. Rossi Albertini, R. Caminiti, F. Cilloco, F. Croce, C. Sadun
Temperature dependence of PEO phase transition rate by energy dispersive X-ray diffraction.
J. Macromol. Sci. Phys. B, 36(2), 221-232 (**1997**).

3) V. Rossi Albertini, G. B. Appetecchi, R. Caminiti, F. Cilloco, F. Croce, C. Sadun
Crystallization kinetics of PEO-alkaline perclorates solutions by energy dispersive X-ray diffraction.
J. Macromol. Sci. Phys. B, 36(5), 623-641 (**1997**).

4) R. Caminiti, L. D'Ilario, A. Martinelli, A. Piozzi and C. Sadun
DSC,FT-IR, and Energy Dispersive X-ray Diffraction Applied to the Study of the Glass Transition of Poly(p-phenylene sulfide).
Macromolecules, 30(25), 7970-7976 (**1997**).

5) V. Rossi Albertini, R. Caminiti, A. Isopo
First measurements by the EDXD-PT technique of the effect of the melting time on polymer crystallisation kinetics.
J. Macromol. Sci. Phys. B, 38(4), 329-339 (**1999**).

6) R. Caminiti, V. Rossi Albertini
Review on the kinetics of phase transitions observed by energy dispersive X-ray diffraction.
Intern. Rev. in Phys. Chem., 18(2), 263 (**1999**).

7) F. Croce, B. Scrosati, L. Persi, F. Ronci, R. Curini, A.Martinelli, R. Caminiti
Physical and chemical properties of nanocomposite polymer electrolytes.
J. Phys. Chem. B, 103(48), 10632-10638 (**1999**).

8) R. Caminiti, A. Isopo, M. A. Orrù, V. Rossi Albertini
Compared EDXD-DSC resolved studies of Poly(ethilene-succinate) multiple melting.
Chem. of Mat., 12, 369-375 (**2000**).

9) R. Caminiti, L. D'Ilario, A. Martinelli, A. Piozzi
Poly(phenylene sulfide) isotermal cold crystallization investigated by usual and unusual methods.
Macromol. Chem. Phys., 202(9), 2902-2914 (**2001**).

10) V. Rossi Albertini, A. Isopo, U. Tentolini and R. Caminiti
Energy dispersive x-ray diffractometry as a tool alternative to differential scanning calorimetry for investigating polymer phase transitions.
Appl. Phys. Lett., 80, 775-777 (**2002**).

11) A. Isopo, V. Rossi Albertini, U. Tentolini and R. Caminiti
Energy dispersive x-ray diffraction and diffrential scanning calorimetry investigation of the melting behavior of poly(ethylene-succinate) crystallized at low undercooling.
J. Appl. Phys., 94(3), 1521-1526 (**2003**).

12) G. Portale, A. Longo, L. D'Ilario, A. Martinelli and R. Caminiti
Energy-dispersive small-angle X-ray scattering for investigating polymer morphology: static and time-resolved experiments.
Appl. Phys. Lett., 85, 4798-4800 (**2004**).

13) V. Rossi Albertini, B. Paci, A. Generosi, M. A. Navarra, S. Panero and M. Di Michiel.
In-situ X-ray diffraction studies of the hydration degree of the polymeric membrane in a fuel cell
Electrochem. Solid State, 7(12), 519-521 (**2004**).

14) A. Martinelli, L. D'Ilario and R. Caminiti
Pol(p-phenylene sulfide) Non-Isothermal Cold-Crystallization.
J. Polym. Sci. Pol. Phys., 43(19), 2725-2736 (**2005**).

CULTURAL HERITAGE

1) R. Caminiti and G. Portale
Analisi delle policromie in frammenti Pesaresi e Faentini mediante Fluorescenza X In "Maioliche del Quattrocento a Pesaro.Frammenti di storia dell'arte ceramica dalla bottega dei fedeli."
(A. Ciarloni) Centro di Firenze, 255-258 (**2004**).

2) P. Ballirano, G. Caracciolo, C. Sadun and R. Caminiti
The use of Energy Dispersive X-ray Diffraction for the investigation of the structural and compositional features of old and modern papers.
Microchem. J., (**2007**) *Submitted*.

3) E. Caponetti, R. Caminiti, D. Chillura Martino and M. L. Saladino
Energy dispersive X-ray diffraction potentiality in the field of Cultural Heritage: simultaneous structural and elemental analysis of various artefacts.
Ann. Chim.-Sci. Mat., (**2007**) *Submitted*.

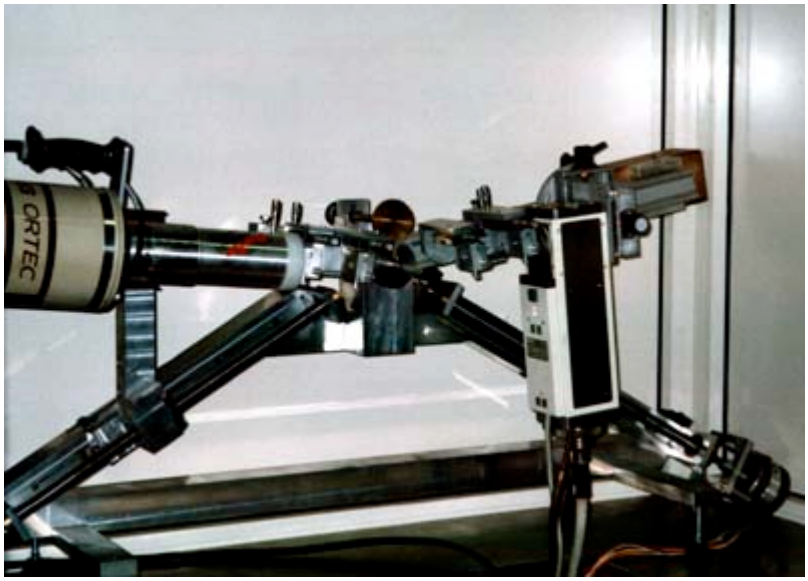

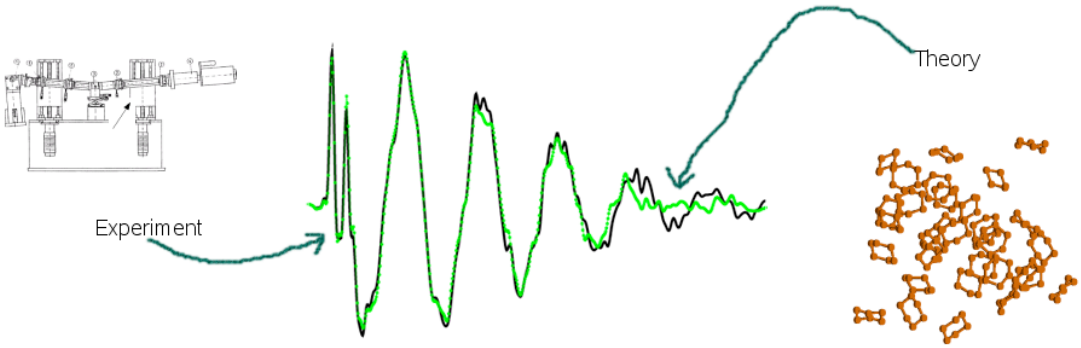

Università degli Studi di Roma Sapienza
Dipartimento di Chimica- Stanislao Cannizzaro
Centro Nazionale Ricerche.
Istituto di Struttura della Materia.
http://www.caminiti.chem.uniroma1.it